

Improved Feature Importance Computations for Tree Models: Shapley vs. Banzhaf*

Adam Karczmarz[†] Anish Mukherjee[‡] Piotr Sankowski[§] Piotr Wygocki[¶]

Abstract

Shapley values are one of the main tools used to explain predictions of tree ensemble models. The main alternative to Shapley values are Banzhaf values that have not been understood equally well. In this paper we make a step towards filling this gap, providing both experimental and theoretical comparison of these model explanation methods. Surprisingly, we show that Banzhaf values offer several advantages over Shapley values while providing essentially the same explanations. We verify that Banzhaf values:

- have a more intuitive interpretation,
- allow for more efficient algorithms,
- are much more numerically robust.

We provide an experimental evaluation of these theses. In particular, we show that on real world instances.

Additionally, from a theoretical perspective we provide new and improved algorithm computing the same Shapley value based explanations as the algorithm of Lundberg et al. [Nat. Mach. Intell. 2020]. Our algorithm runs in $O(TLD + n)$ time, whereas the previous algorithm had $O(TLD^2 + n)$ running time bound. Here, T is the number of trees, L is the maximum number of leaves in a tree, and D denotes the maximum depth of a tree in the ensemble. Using the computational techniques developed for Shapley values we deliver an optimal $O(TL + n)$ time algorithm for computing Banzhaf values based explanations. In our experiments these algorithms give running times smaller even by an order of magnitude.

*All authors were supported by the ERC Consolidator Grant 772346 TUgBOAT.

[†]University of Warsaw, a.karczmarz@mimuw.edu.pl

[‡]University of Warsaw, anish@mimuw.edu.pl

[§]IDEAS NCBR, University of Warsaw, and MIM Solutions, Warsaw, sank@mimuw.edu.pl

[¶]University of Warsaw, and MIM Solutions, Warsaw, wygos@mimuw.edu.pl. Additionally supported by the Polish National Science Center Grant PRELUDIM 2018/29/N/ST6/00676.

1 Introduction

The explainability of machine learning models has become one of the crucial aspects when deploying such models in practice. When high-value decisions are taken, understanding why a model made a certain prediction is even more important than the prediction’s accuracy. In such applications, e.g., medical diagnostic, taking into account the necessity of human oversight is a must. Thus we need to deliver methods that would interpret the model’s results, so that humans are actually willing to follow model recommendations.

As a result, recently there has been a growing interest in feature attribution problems, where one would like to distribute the prediction of a model f to the individual features used in the model. The feature attributions are used to explain the relative influence of individual features to the model’s prediction $f(x)$ on some specific input x .

Feature influence. The most popular approaches to interpreting model predictions is based on so-called *Shapley values* (e.g., [31, 33, 51, 53]). The attractiveness of this approach comes from the fact that Shapley values can be very efficiently computed in the case of tree ensemble models. Although some papers suggest using Banzhaf values [14, 49, 36] in place of Shapley values, this alternative has not been understood equally well.

In general, the motivation for using the Shapley/Banzhaf values in this context comes from game theory. Their use is justified by the fact that they are known to be the unique method of measuring the importance, or value, of a player in a coalitional game $g : 2^U \rightarrow \mathbb{R}$, that satisfies a certain set of desirable axioms which differ slightly for Shapley and Banzhaf values. Here, g gives an utility of a coalition, $g(\emptyset) = 0$ and U is the set of players (or – in our context – features).

However, as explained in [52], despite the uniqueness of Shapley values, many different Shapley values-based attribution methods have been studied. This is because, we need to define a *set function* g that extends f to all subset of features $S \subseteq U$, i.e., g allows us to drop features $U \setminus S$ of x . Given such a set function g , and $n = |U|$, the Shapley value of the feature $i \in U$ is defined:

$$\phi_i = \frac{1}{n} \sum_{S \subseteq U \setminus \{i\}} \binom{n-1}{|S|}^{-1} (g(S \cup \{i\}) - g(S)). \quad (1)$$

Let us mention some concrete examples of g used in [22, 31, 52]. In the *Baseline Shapley* approach (BShap), some baseline feature vector $x' \in \mathbb{R}^U$ is given. Then for any $S \subseteq U$ $g(S) := f(x_S, x'_{U \setminus S}) - f(x'_U)$, where $f(x_S, x'_S)$ is the output of the model for a feature vector whose feature values for features in S are taken from x , whereas the values for features in $U \setminus S$ are taken from x' .

In the *Marginal Expectation Shapley* approach (MES), $g(S) := \mathbb{E}[f(x_S, X_{U \setminus S})] - \mathbb{E}[f(X_U)]$, where X_V denote the random variables corresponding to the values of features in $V \subseteq U$. Similarly, in the *Conditional Expectation Shapley* approach (CES), $g(S) := \mathbb{E}[f(X_U) | X_S = x_S] - \mathbb{E}[f(X_U)]$.

We note that explanations based on Shapley values have been extensively studied experimentally [31, 33, 51, 53], whereas in the case of Banzhaf values such study was only done on single data sets [14, 49, 36]. Moreover, despite very high similarity of both methods, only limited experimental comparison between them can be found in the literature. We are only aware of the recent comparison of the both methods in [36], which is limited to a single depth-3 tree. We review other methods in Section 8.

This paper aims to make a step towards filling this gap by providing theoretical as well as experimental commissional study of these methods. In particular, our contribution is the first to clearly visualize that for tree ensemble models, Banzhaf values:

- have a more intuitive interpretation – they correspond directly to the probability that a model prediction changes when changing a feature,
- allow for more efficient algorithms – in our experiments the speed-up is by an order of magnitude,
- are much more numerically robust – we observe that due to numerical errors, using Shapley values can lead to a wrong ordering of features.

Thus our paper adds new cardinal arguments towards usage of Banzhaf values for feature attribution.

Computational complexity. In general, computing Shapley and Banzhaf values is a computationally hard problem [16, 34]. With just a black-box access to the set function, it seems that a naive evaluation of the formula (1) is the best we can hope for. However, for some specific models f and choices of the set function, Shapley values can be computed much faster.

One of the main contributions of Lundberg et al. [31] was to show efficient algorithms computing Shapley values for binary tree ensemble models for two different plausible set functions g (see Section 2). One of these algorithms, called TREESHAP_PATH [31, Algorithm 2], is particularly interesting and convenient; it provides explanations without the help of the background dataset. Instead, it uses a set function based on subtree coverages (see Algorithm 1) proposed in the classical work Friedman [19] for estimating partial dependence plots. The algorithm runs in $O(TLD^2 + n)$ time, where T is the number of trees, L is the maximum number of leaves in a tree, and D denotes the maximum depth of a tree in the ensemble. Note also that using Equation (1) naively would take exponential $\Omega(TnL \cdot 2^n)$ time in this case. As noted in [36], the same algorithm applies to Banzhaf values.

Our first contribution is a new algorithm computing the same explanation of a tree ensemble model prediction as the TREESHAP_PATH algorithm of Lundberg et al. [31]. The algorithm is asymptotically even faster and runs in $O(TLD + n)$ time. We demonstrate that for trees of depth $\text{apx. } 20$ it outperforms the original algorithm. Applying the same techniques to Banzhaf values we are able to obtain even faster algorithm running in $O(TL + n)$ time.

1.1 Axioms, Efficiency, and Power Indices

As already mentioned, the use of Shapley values for attribution is a must if we want the attribution to satisfy some natural axioms: *Efficiency*, *Sensitivity*, *Linearity*, and *Symmetry*. For their precise definition¹, consult [22, 52]. The efficiency axiom is particularly interesting. It says that the sum of individual attributions $\sum_{i \in U} \phi_i$ should equal exactly $g(U)$. In all the known approaches for defining g (cf. [52]), $g(U)$ equals precisely the difference between the prediction and some baseline. As argued in [53], efficiency “*is a sanity check that the attribution method is somewhat comprehensive in its accounting, a property that is clearly desirable if the score is used in a numeric sense, and not just to pick the top label, for e.g., a model estimating insurance premiums from credit features of individuals*”. However, the cost of this mathematical property is a rather nonintuitive meaning of these values. In order to guarantee efficiency, one needs to weight the contribution of each feature with the total number of orderings of the present as well as the absent features as given by (1). It is rather unclear why feature vector $(man, 40)$ is different from $(40, man)$, and why this should matter for feature importance.

This nonintuitive aspect becomes clearly visible when moving out of the cost-sharing regime to the study of voting power indices. Applying this concept to model explanation, power indices essentially measure the

¹*Sensitivity* axiom is sometimes called the *dummy/null player* axiom, whereas *efficiency* is also called *completeness*.

voting power of a particular feature on the decision taken by the model. There are several options for power indices with two being dominating ones: the Shapley-Shubik power index and the Banzhaf power index. In some cases, Banzhaf index works better [28] whereas in others Shapley-Shubik [8]. Shapley-Shubik index uses Shapley values (1), whereas Banzhaf index attributes *Banzhaf values* β_i defined:

$$\beta_i = \frac{1}{2^{n-1}} \sum_{S \subseteq U \setminus \{i\}} g(S \cup \{i\}) - g(S). \quad (2)$$

Different axiomatic parameterizations have been given for both concepts, see e.g. [27], and different paradoxes (i.e., nonintuitive properties) were found [24]. Compared to Shapley values, Banzhaf values satisfy *Sensitivity*, *Linearity*, and *Symmetry*, but not *Efficiency*. This axiom is replaced by the *2-Efficiency* axiom [29]. When studying power indices, the efficiency axiom is not considered as a must which is the case in cost-sharing games [20]. This axiomatic approach has been followed in [33, 14, 49, 36], and analogous axiomatizations have been proven for feature values based on these concepts.

We note, however, that in the case of power-indices the discussion on different options is rather complex [17]. In general, one points out that aspects other than existence of axioms should be used to decide which power index to use [25]. Moreover, it is argued that “axiomatic approach by itself is insufficient to settle the question of the choice of a power index” [26], i.e., the consequences of different axioms can be rather non-intuitive and axioms that seem to be the most basic ones can lead to paradoxes [24]. Laruelle [26] suggests that in order to choose between Banzhaf and Shapley probabilistic approach could be followed. In this interpretation, Shapley index can be used when the order of players/features matters, whereas Banzhaf values should be used when this order is not important. Nevertheless, it is observed that both methods deliver very similar results, and one usually computes both when doing experimental evaluations – as in [28, 8]. Moreover, it has been formally proven that Banzhaf and Shapley-Shubik indices are consistent when applied to restricted voting systems [35], i.e., return the same ordering of players. These observations motivated us to formulate the following hypothesis.

Hypothesis 1. *Banzhaf and Shapley values lead to the same ordering of features for tree ensemble models.*

We note that a priori it is unclear whether the above could be true, as the above observations hold for voting systems which satisfy much more properties than decision models considered here.

1.2 Banzhaf Values vs Shapley Values

The main contribution of this paper is to fill in the experimental gap, by providing study of Shapley and Banzhaf values on tree ensemble models. In particular, we experimentally verify Hypothesis 1 and show that both methods deliver essentially the same average importance scores for the four studied datasets. Moreover, we prove that for monotone functions on a hypercube both measure give the same ordering. Hence, differences in axiomatic definitions do not seem to actually deliver the answer on which index to use. Even though Banzhaf values do not obey the efficiency axiom, we argue that they have several important advantages over Shapley values when applied to feature importance measurement.

Intuitive meaning. As pointed out in the power index literature [18], many researchers believe that the main advantage of Banzhaf values is their more intuitive definition. In the voting setting, the Banzhaf power index is defined as the *expected change to the model output when a given vote is added*. In order to define the Shapley-Shubik power index, one considers an ordered process of forming voter lists, i.e., one adds players one by one to the ordered list and computes how often a given voter changes the outcome. When

reinterpreting the Banzhaf power index in the machine learning model setting, one essentially obtains that a Banzhaf value corresponds to the expected change of the model prediction when a given feature is added. As argued above, using Shapley values does not allow for such a straightforward interpretation.

Computational efficiency. As for Shapley values, in general, computing Banzhaf values requires exponential time [40]. However, we show that Banzhaf values are tailored to work with tree ensemble models even better than Shapley values. The TREESHAP_PATH explanation algorithm of Lundberg [31], adjusted to compute Banzhaf values instead (when using the same natural set function g) has running time $O(TLD+n)$, which constitutes a factor- D speedup over the Shapley-based version. More importantly, with the new ideas that we use to speed-up the TREESHAP_PATH algorithm, we are able to obtain an $O(TL+n)$ time algorithm for computing Banzhaf values for this choice of g . Note that this algorithm is *asymptotically optimal*, since even the description of a tree ensemble has size $O(TL)$, and the output has size $O(n)$. In experiments, this algorithm visibly outperforms all other algorithms based on that set function, and can lead to considerable time saving when computing feature importance values for decision tree-based models in practice.

We note that other Shapley values-based algorithm for trees proposed in [31] (TREESHAP_INT) can be also easily modified to yield Banzhaf values instead within the same time bound.

Numerical accuracy. While experimenting with different implementations of Shapley value-based explanations for tree ensemble models, we have observed that the results obtained using different implementations are different. These observations are discussed in Section 5.3. We note that an implementation that would use single numerical precision would be essentially useless, whereas for double precision differences in ordering of features can be seen for trees of depth 4 (NHANES_GBDT instance, the difference in ordering within the first 10 features). Moreover, we provide a very simple synthetic example of non-balanced trees showing that for depth apx. 50 numerical errors would dominate the result. Trees of even higher depth are sometimes used in practice [54].

Banzhaf values, due to a simpler definition, are here much more robust and only very small errors are visible in the computations. Essentially, for trees considered in our experiments, numerical errors are not observable. This is further illustrated on the synthetic example where numerical errors of Banzhaf method are negligible.

Approximate equivalency. In our experimental evaluation, we show that in practice the Banzhaf and Shapely values give approximately the same feature importance. For three instances, the ordering of the mean absolute values for the top 20 most important features was the same (Figures 2, 3, 4). Usually, the ordering of features is very similar, e.g., for three datasets it is enough to perform a single swap on average on the first 10 features to change Shapley-based feature ordering to Banzhaf-based ordering (see Table 1). In Section 5.5, we present a comparison for mean average error and root mean square error for measuring the distance between Shapley values and Banzhaf values. Moreover, we show the worst-case comparison.

In our opinion, these arguments indicate that for tree models, Banzhaf values should be preferred in practical applications. Both methods deliver comparable explanations, but Banzhaf values work faster and are much less prone to numerical errors.

From the theoretical perspective, we consider monotone functions on a hypercube, i.e., functions that for a given feature i and any feature vector x , setting $x_i := 1$ (similarly $x_i := 0$) is either always increasing (or always decreasing) our value function. We prove that for such functions and uniform distribution of the

dataset, any power index in the form:

$$\sum_{S \subseteq U \setminus \{i\}} w(S) (g(S \cup \{i\}) - g(S)),$$

for a distribution $w : 2^U \rightarrow \mathbb{R}$, $\sum_{S \subseteq U} w(S) = 1$, gives exactly the same mean absolute importance of features. In particular, this shows that for some natural instances using Banzhaf and Shapley values for computing global feature importance is equivalent. See Section 4 for more details.

2 Preliminaries

Let $U := \{1, \dots, n\}$ be a set of *features*. Let x generally denote a *feature vector*, i.e., x is formally a function $x : U \rightarrow \mathbb{R}$. For $i \in U$, we write x_i to refer to the *value* of i -th feature in x . More generally, for any subset $S \subseteq U$ we write x_S when referring to the function $x|_S$. We sometimes talk about random feature vectors, or consider the values of individual features as random variables. We then write X or X_i respectively. We write X_S to denote the set of random variables $\{X_i : i \in S\}$. Let \bar{S} denote the complement $U \setminus S$. Let $f : \mathbb{R}^U \rightarrow \mathbb{R}$ be the output function of our model.

Trees. We focus on tree ensemble models, where the output of the model is simply the average output of its T individual trees. For simplicity, we assume $T = 1$ but still incorporate the variable T when stating the time complexities (as done in [31]): the algorithms we discuss run independent computations for all the trees in the ensemble. Also, we assume the individual trees are roughly of the same size and depth.

When talking about the input decision tree \mathcal{T} , we adopt the notation of [31]. \mathcal{T} is a binary tree based on single-variable splits: each non-leaf node $v \in \mathcal{T}$ is assigned a *feature* d_v , and a *threshold* t_v , whereas each leaf l is assigned a *value* $f(l)$. Let a_v, b_v denote the left and right children of a non-leaf node $v \in \mathcal{T}$. The output $f(x)$ is computed by following a root-leaf path in \mathcal{T} : at a non-leaf node $v \in \mathcal{T}$, we descend to a_v if $x_{d_v} < t_v$, or to b_v otherwise. When a leaf is reached, its value is returned. Denote by $\mathcal{L}(\mathcal{T})$ the set of leaves of \mathcal{T} . Denote by $\mathcal{T}[v]$ the subtree of v rooted at v . Let L and D denote the number of leaves and the depth of the tree \mathcal{T} , resp.

Set functions and Shapley values. We write $f(x_S, X_{\bar{S}})$ when referring to a random variable defined as the value of f if the values for features in S are fixed to the respective values of x , and the values $X_{\bar{S}}$ are random variables. Let X_U be distributed as in the training set.

Given a *set function* $g : 2^U \rightarrow \mathbb{R}$ with $g(\emptyset) = 0$, the Shapley values ϕ_i for $i \in U$ are defined as in Equation (1).

Lundberg et al. [31] and Janzing et al. [22] suggest using the following idealized set function g^* for feature attribution:

$$g^*(S) := \mathbb{E}[f(x_S, X_{\bar{S}})] - \mathbb{E}[f(X_U)]. \quad (3)$$

Note how the term $\mathbb{E}[f(X_U)]$ in (3) cancels out when computing Shapley values from Equation (1). Thus, for simplicity in the following we can redefine $g^*(S) := \mathbb{E}[f(x_S, X_{\bar{S}})]$.

Using the idealized set function g^* would be computationally too costly. Consequently, Lundberg et al. [31] considers two different set functions that “approximate” g^* .

In the TREESHAP_PATH algorithm, the approximation $g(S) \approx g^*(S)$ is computed using Algorithm 1. This method dates back to the classical work of Friedman [19] and is also implemented as a way to compute partial dependence plots in the scikit-learn package [37]. Its one advantage is that it does not require access

to the training data, but merely to the “coverages” r_v of all the subtrees $\mathcal{T}[v]$, i.e., the numbers of training set points that fall into $\mathcal{T}[v]$. It can be proved that this method computes $\mathbb{E}[f(x_S, X_{\bar{S}})]$ if the individual feature random variables X_i are independent. With such a set function g , Lundberg et al. [31] show how to compute Shapley values ϕ_i exactly in $O(TLD^2 + n)$ time.

On the other hand, in the TREESHAP_INT algorithm, Lundberg et al. [31] estimate $g^*(S)$ by sampling some number R of random points x' of the training data and computing the average value of $f(x_S, x'_{\bar{S}})$ over these samples.² Note that if the entire data was sampled, this would compute the desired expectation exactly. The computation cost would be then unacceptable, though. The TREESHAP_INT algorithm computes the Shapley values ϕ_i exactly (for the described approximation of g^*) in $O(TRL + n)$ time. We stress that this method requires access to the training data.

In the remaining part of the paper, we denote by $g(S)$ the output of Algorithm 1 for the subset $S \subseteq U$, i.e., we consider the same approximation of $g^*(S)$ as in the TREESHAP_PATH algorithm of [31].

3 Improved Algorithm: Outline

In this section we sketch an improved algorithm computing the same Shapley value explanations as the TREESHAP_PATH algorithm that takes $O(TLD + n)$ time in the worst case. As we later show, the improvement is indeed noticeable experimentally for unbalanced decision trees with large depth.

Let us first describe the idea behind the $O(LD^2 + n)$ time algorithm of Lundberg et al. [31] for $T = 1$. To this end, we need to fix some more notation. Let ρ be the root of \mathcal{T} . Let p_v denote the parent of a node $v \in \mathcal{T}$, $v \neq \rho$. Let F_v be the set of features assigned to the ancestors of v , i.e., $F_\rho = \emptyset$, and $F_v = F_{p_v} \cup \{d_{p_v}\}$ for $v \neq \rho$. The value $P[v] = r_v/r_\rho$ can be thought as the probability that the model returns a value from the subtree of v . Moreover, note that the output of Algorithm 1 for $S = \emptyset$ is precisely equal to $\sum_{l \in \mathcal{L}(\mathcal{T})} P[l] \cdot f(l)$. More generally, denote by $P[v, S]$ the weight from the ancestor recursive calls assigned to the subtree rooted at v when running Algorithm 1 with an arbitrary subset $S \subseteq U$. Formally, $P[\rho, S] = 1$, and for any $v \neq \rho$,

$$P[v, S] = \begin{cases} P[p_v, S] \cdot \frac{r_v}{r_{p_v}} & \text{if } d_{p_v} \notin S, \\ P[p_v, S] \cdot [x_{d_{p_v}} < t_{p_v}] & \text{if } d_{p_v} \in S, v = a_{p_v}, \\ P[p_v, S] \cdot [x_{d_{p_v}} \geq t_{p_v}] & \text{if } d_{p_v} \in S, v = b_{p_v}. \end{cases}$$

Then, the algorithm outputs

$$\sum_{l \in \mathcal{L}(\mathcal{T})} P[l, S] \cdot f(l) = g(S) \approx g^*(S) = \mathbb{E}[f(x_S, X_{\bar{S}})]. \quad (4)$$

First of all, each value ϕ_i is obtained by summing the contributions of each individual leaf $l \in \mathcal{L}(\mathcal{T})$ with $i \in F_l$ to the sum (1) with g defined as in (4).³ This is in turn achieved as follows. For any subset $G \subseteq U$, let

$$\phi(v, G, k) := \frac{1}{|G| + 1} \sum_{\substack{S \subseteq G \\ |S|=k}} \binom{|G|}{k}^{-1} \cdot P[v, S].$$

²In [52] this method is called *Random Baseline Shapley*.

³If $i \notin F_l$ then it can be shown that the contribution of l to ϕ_i is 0. This is also why the TREESHAP_PATH algorithm’s dependence on n is just $O(n)$.

Algorithm 1 Estimating $\mathbb{E}[f(x_S, X_{\bar{S}})]$.

function Desc(S, v)
1: **if** $v \in \mathcal{L}(\mathcal{T})$ **then**
2: **return** $f(v)$
3: **else**
4: **if** $d_v \in S$ **then**
5: **return** (**if** $x_{d_v} < t_v$ **then** Desc(S, a_v) **else** Desc(S, b_v))
6: **else**
7: **return** $\frac{1}{r_v} \cdot (r_{a_v} \cdot \text{Desc}(S, a_v) + r_{b_v} \cdot \text{Desc}(S, b_v))$
function $g(S)$
1: **return** Desc(S, ρ)

Let us call the following vector of values a *state* for (v, G) :

$$\Psi(v, G) = (\phi(v, G, k))_{k=0}^{|G|}$$

One can prove that moving between “nearby” states can be performed efficiently. Namely, given $\Psi(v, G)$, in $O(|G|)$ time one can compute each of the states: $\Psi(p_v, G)$, $\Psi(a_v, G)$, $\Psi(b_v, G)$, $\Psi(v, G \cup \{i\})$, $\Psi(v, G \setminus \{i\})$, for any feature $i \in U$.

Let $\phi(v, G) = \sum_{k=0}^{|G|} \phi(v, G, k) = \|\Psi(v, G)\|_1$. Clearly, given $\Psi(v, G)$, $\phi(v, G)$ can be obtained easily in $O(|G|)$ time. One can show that the individual contribution of leaf l to ϕ_i for $i \in F_l$ equals

$$f(l) \cdot (\phi(l, F_l) - \phi(l, F_l \setminus \{i\})) \tag{5}$$

Using our notation, the algorithm of Lundberg et al. does the following. First, all states $\Psi(v, F_v)$ for $v \in \mathcal{T}$ are computed using a simple recursive tree traversal in time

$$O\left(\sum_{v \in \mathcal{T}} |F_v|\right) = O\left(\sum_{l \in \mathcal{L}(\mathcal{T})} |F_l|\right) = O(LD),$$

since one can obtain $\Psi(v, F_v)$ from $\Psi(p_v, F_{p_v})$ in $O(|F_v|) = O(D)$ time. This also gives all the values $\phi(l, F_l)$ that we need when computing leaf contributions using (5). Afterwards, for each leaf $l \in \mathcal{T}$, all the $|F_l|$ states $\Psi(l, F_l \setminus \{i\})$ for $i \in F_l$ can be computed in $O(|F_l|)$ time each. Given such a state, the leaf l 's contribution to ϕ_i can be computed in $|F_l|$ time as well. As a result, through all pairs (l, i) , this takes $O\left(\sum_{l \in \mathcal{L}(\mathcal{T})} |F_l|^2\right) = O(LD^2)$ time. The algorithm sketched above is described in detail in Section 6.

The general idea behind our improved algorithm is to avoid computing all the leaf contributions to each ϕ_i separately. Instead, for a node $v \in \mathcal{T}$ with $d_v = i$, we compute the total contribution to ϕ_i of all leaves $\mathcal{L}_v \subseteq \mathcal{T}[v]$ for which v constitutes the nearest ancestor with $d_v = i$ at once. To this end, we show that, roughly speaking, we can “remove” a feature i from the sum $\Phi(v) := \sum_{l \in \mathcal{L}_v} f(l) \cdot \phi(l, F_l)$ of all the leaf states in the subtree $\mathcal{T}[v]$ (and thus obtain the sum $\sum_{l \in \mathcal{L}_v} f(l) \cdot \phi(l, F_l \setminus \{i\})$) in $O(D)$ time as well. This in turn allows us to get the second step of the algorithm in [31] replaced with a bottom-up computation with $O(LD)$ cost.

Actually, our improvement requires some more technical care and only works if all the sets F_l have a uniform size h . However, a binary tree with all sets F_l having the same size h has $\Theta(2^h)$ leaves and thus padding the tree with “dummy” leaves would be too costly. To deal with this problem, we instead consider states $\Psi(l, F_l^*)$ where $F_l^*, F_l \subseteq F_l^*$, is the set F_l padded with $h - |F_l|$ “dummy” features that do not appear in the tree’s nodes at all. Details can be found in Section 7.

Banzhaf Values for Trees The importance of individual features for a single prediction using the *Banzhaf values* are defined as in Equation (2). Recall that we fixed g to be the same approximation of g^* that we used in the previous section. In Section 6.3 we show that for this particular set function g , the Banzhaf values as defined in (2) can be computed using an algorithm analogous to TREESHAP_PATH of [31] in $O(LD)$ time. Moreover, by applying our optimization to the TREESHAP_PATH algorithm, the time bound can be further reduced to optimal $O(L)$. Intuitively, this is possible since the coefficients of individual terms $g(S \cup \{i\}) - g(S)$ in the sum (2) do not depend on the size $|S|$. As a result, an analogously defined *state* $\beta(v, G)$ consists of only one value:

$$\beta(v, G) := \frac{1}{2^{|G|}} \sum_{S \subseteq G} P[v, S],$$

and one can again “move” between the “nearby” states in $O(1)$ time, as opposed to $O(L)$ time which was the case for the Shapley values computation.

4 Monotone Functions on Hypercube

In this section we give an idealized example that sheds some light on why Shapley and Banzhaf values can agree on some datasets. Essentially, when the dataset gets close to the uniform case, i.e., many configurations of features are present, we should see that both importance measures are equal. More formally, let $U = \{1, \dots, k\}$, and let \mathcal{D} be some dataset. Suppose for each $i \in U$ we have some feature attribution function $\gamma_i : \mathcal{D} \rightarrow \mathbb{R}$. Let us consider the *global impact* of the feature over dataset \mathcal{D} measured as

$$\Gamma_i = \sum_{x \in \mathcal{D}} |\gamma_i(x)|.$$

For example, we can set $\gamma_i = \phi_i$ to get a *Shapley global impact* Φ_i , or we can set $\gamma_i = \beta_i$ to get a *Banzhaf global impact* B_i . This measure of global feature importance has also been used by Lundberg et al. [31].

In this section, we consider the set of *monotone* functions on uniformly-distributed vertices of a k -dimensional hypercube and show that the Shapley global impacts and the Banzhaf global impacts always agree on them. When defining Shapley and Banzhaf values we use the idealized set function $g_x^*(S) = \mathbb{E}[f(x_S, X_{\bar{S}})]$ as in Section 2.

More precisely, let the considered dataset be $\mathcal{D} = \{0, 1\}^k$ and the data is spread uniformly, i.e., for each a random variable $X \in \mathcal{D}$, we have $\mathbb{P}[X = x] = 2^{-k}$ for all $x \in \mathcal{D}$. For a subset of indices S and a vector $x \in \{0, 1\}^k$ let $\mathcal{D}_{S,x}$ be the set of all points in \mathcal{D} which matches x on the set S , i.e., $\mathcal{D}_{S,x} = \{x' | x' \in \mathcal{D}, x'_S = x_S\}$.

Let $f : \mathcal{D} \rightarrow \mathbb{R}$ be a function. Let x^{-i} denote x with the value of feature i flipped to the opposite value. We say that f is monotone in feature i if for each $\alpha \in \{0, 1\}$ all the numbers in the set $\{f(x) - f(x^{-i}) | x \in \mathcal{D}, x_i = \alpha\}$ have the same sign.

Let $w : 2^U \rightarrow \mathbb{R}_{\geq 0}$ be a *coefficient function* such that for any $i \in U$, we have $\sum_{S \subseteq U \setminus \{i\}} w(S) = 1$. For data point $x \in \mathcal{D}$, we define the w -value of a feature i as follows:

$$\omega_i^w(x) = \sum_{S \subseteq U \setminus \{i\}} w(S) \cdot (g_x^*(S \cup \{i\}) - g_x^*(S)).$$

Observe that the appropriate choice of the coefficient function w can yield Shapley values, Banzhaf values, or, e.g., probabilistic values [55]. Moreover, let the total w -impact be $\Omega_i^w = \sum_{x \in \mathcal{D}} \omega_i^w(x)$.

In our settings, we have:

$$g_x^*(S) = \mathbb{E}[f(x_S, X_{\bar{S}})] = \sum_{x' \in \mathcal{D}_{S,x}} \frac{f(x')}{|\mathcal{D}_{S,x}|}$$

Now we prove that the impacts Ω_i^w for $i \in U$ are independent of the coefficient function w for our choice of \mathcal{D} , the uniform distribution, and monotone functions $f : \mathcal{D} \rightarrow \mathbb{R}$. This will prove that for all $i \in U$, $\Phi_i = B_i$.

We have:

$$\begin{aligned} \omega_i^w(x) &= \sum_{S \subseteq U \setminus \{i\}} w(S) \cdot (g_x^*(S \cup \{i\}) - g_x^*(S)) \\ &= \sum_{S \subseteq U \setminus \{i\}} w(S) \left(\sum_{x' \in \mathcal{D}_{S \cup \{i\}, x}} \frac{f(x')}{|\mathcal{D}_{S \cup \{i\}, x}|} - \sum_{x' \in \mathcal{D}_{S,x}} \frac{f(x')}{|\mathcal{D}_{S,x}|} \right) \\ &= \sum_{S \subseteq U \setminus \{i\}} w(S) \left(\sum_{x' \in \mathcal{D}_{S \cup \{i\}, x}} \frac{f(x')}{2^{k-|S|-1}} - \sum_{x' \in \mathcal{D}_{S,x}} \frac{f(x')}{2^{k-|S|}} \right) \\ &= \sum_{S \subseteq U \setminus \{i\}} w(S) \cdot 2^{|S|-k} \left(\sum_{x' \in \mathcal{D}_{S \cup \{i\}, x}} 2f(x') - \sum_{x' \in \mathcal{D}_{S,x}} f(x') \right) \\ &= \sum_{S \subseteq U \setminus \{i\}} w(S) \cdot 2^{|S|-k} \left(\sum_{x' \in \mathcal{D}_{S \cup \{i\}, x}} f(x') - f(x'^{-i}) \right). \end{aligned}$$

By the monotonicity of f , we get:

$$|\omega_i^w(x)| = \sum_{S \subseteq U \setminus \{i\}} w(S) \cdot 2^{|S|-k} \left(\sum_{x' \in \mathcal{D}_{S \cup \{i\}, x} } |f(x') - f(x'^{-i})| \right).$$

Now we are ready to compute Ω_i^w . By changing the order of summation, we get:

$$\begin{aligned} \Omega_i^w &= \sum_{x \in \mathcal{D}} |\omega_i^w(x)| \\ &= \sum_{S \subseteq U \setminus \{i\}} w(S) \cdot 2^{|S|-k} \sum_{x \in \mathcal{D}} \left(\sum_{x' \in \mathcal{D}_{S \cup \{i\}, x}} |f(x') - f(x'^{-i})| \right) \\ &= \sum_{S \subseteq U \setminus \{i\}} w(S) \cdot 2^{|S|-k} \sum_{x' \in \mathcal{D}} |f(x') - f(x'^{-i})| \cdot |\{x : x' \in \mathcal{D}_{S \cup \{i\}, x}\}| \end{aligned}$$

Now note that for a fixed $x' \in \mathcal{D}$, x' is present in the set $\mathcal{D}_{S \cup \{i\}, x}$ for $2^{k-|S|-1}$ distinct points $x \in \mathcal{D}$.

Hence:

$$\begin{aligned}
\Omega_i^w &= \sum_{S \subseteq U \setminus \{i\}} w(S) \cdot 2^{|S|-k} \sum_{x' \in \mathcal{D}} |f(x') - f(x'^{-i})| \cdot 2^{k-|S|-1} \\
&= \frac{1}{2} \sum_{S \subseteq U \setminus \{i\}} w(S) \cdot \left(\sum_{x \in \mathcal{D}} |f(x) - f(x^{-i})| \right) \\
&= \frac{1}{2} \left(\sum_{x \in \mathcal{D}} |f(x) - f(x^{-i})| \right) \cdot \left(\sum_{S \subseteq U \setminus \{i\}} w(S) \right) \\
&= \frac{1}{2} \sum_{x \in \mathcal{D}} |f(x) - f(x^{-i})|.
\end{aligned}$$

The last equality follows since the coefficients $w(S)$ for $S \subseteq 2^U$ add up to 1. Thus Ω_i^w is independent of w . It follows that $\Omega_i^w = \Phi_i = B_i$ for all $i \in U$, which completes the proof.

5 Experimental Results

5.1 Datasets

In our experiments, we used six datasets: four real and two artificial. These datasets were obtained by running either the sklearn implementation of Decision Trees (DT) or xgboost implementation of Gradient Boosting Decision Trees (GBDT) on three predictions datasets. These are some of the most popular algorithms for generating decision trees and are quite often used for large depths of the trees. Using large-depth trees is particularly beneficial for datasets with many features and complex relationship between features (see e.g., [9, 38] for a usage of trees of depth 100). Let us emphasize that the large depth of the tree e.g. height 100 does not mean that the size of the tree is 2^{100} , because trees might be (and usually are) unbalanced. To simplify the experiments and reduce the running times of experiments we trained the DT algorithm for only one tree. The algorithm's parameters and the basic dataset's descriptions are as follows:

1. **BOSTON** [1]. This small prediction dataset contains information concerning housing in the area of Boston Massachusetts. The task is to predict the price of the house. The dataset contains 506 rows and 13 columns. The decision tree (DT) was trained with `tree_depth` equal to 10, all of the other parameters are set set to default values. The parameters used for training xgboost were: 100 iterations, max depth 6, and learning rate equal to 0.01.
2. **NHANES**. The same dataset that was used in previous work on model interpretability [31]. The dataset contains 8023 rows and 79 columns. The parameters used for training were the same as in the original paper. The DT algorithm was trained with `tree_depth` equal to 40, all of the other parameters are set to default values. The parameters used for training xgboost were: 250 iterations, max depth 4 and learning rate equal to 0.2.
3. **HEALTH_INSURANCE** [3]. A medium size dataset for predicting who might be interested in health insurance. The dataset contains 304887 rows and 14 columns. The DT algorithm was trained with `tree_depth` equal to 60, all of the other parameters are set set to default values. The parameters used for training xgboost were: 250 iterations, max depth 4 and learning rate equal to 0.2.

4. **FLIGHTS** [2]. A large dataset for predicting the flights’ delays. The dataset contains 1543718 rows and 647 columns. The large number of columns was caused by one-hot encoding ’UniqueCarrier’, ’Origin’, ’Dest’, ’CancellationCode’ in a standard way, i.e., for each possible value v of a given column c we created additional categorical column c_v (with a value from $\{0, 1\}$) indicating that the value of c equals v iff the value of c_v equals 1. The DT algorithm was trained with `tree_depth` equal to 100, all of the other parameters are set to default values. The parameters used for training `xgboost` were: 250 iterations, max depth 10, and learning rate 0.2.

The algorithms were not extensively tuned since the main goal is interpreting models not optimizing them. The large trees are used mainly for comparing running times and elucidate numerical problems. We will refer to the above datasets by adding “DT” and “GBDT” suffixes to the ordinal name of the prediction dataset.

We also prepared two synthetic instances with known exact answers (for both Shapley and Banzhaf values):

1. **SYNTHETIC.DENSE**. This instance contains one tree and one data point $x = [1, \dots, 1] \in \mathbb{R}^d$. The tree consists of two subtrees of the same shape, both of them being full binary trees of depth $d - 1$. All values in the leaves are equal to 0 and 777 in left and right subtree respectively. All leaves have coverages equal to 33. In the internal nodes at depth i of the tree we split on the condition $x_{d-i} < 1$ where the set of features is $U = \{1, \dots, d\}$.
2. **SYNTHETIC.SPARSE**. This instance differs from the dense version only with the shape of the subtrees. Here each inner node of subtree has one leaf child and one non-leaf child.

The only feature with a nonzero Shapley/Banzhaf value is the feature d used to split at depth 0. All the other features have zero Shapley/Banzhaf values by the *Sensitivity* axiom.

5.2 Algorithms

In our experiments, we have tested four implementations of algorithms:

- `shap_orig_a` – our implementation of the $O(TLD^2)$ -time algorithm computing Shapley values based on [31],
- `shap_fast` – an implementation of our asymptotically faster $O(TLD)$ -time Shapley values algorithm,
- `shap_orig` – implementation of the `TREESHAP_PATH` algorithm [31] from the SHAP package [4],
- `ban` – an implementation of our $O(TL)$ -time algorithm computing Banzhaf values for tree ensemble models.

The implementations `shap_orig_a` and `shap_fast` are consistent, i.e., produce the same results. There are small differences between `shap_orig` and our implementations of Shapley values but the mean average percentage difference between values is less than 1%. We suspect that these differences are due to numerical differences in implementations.

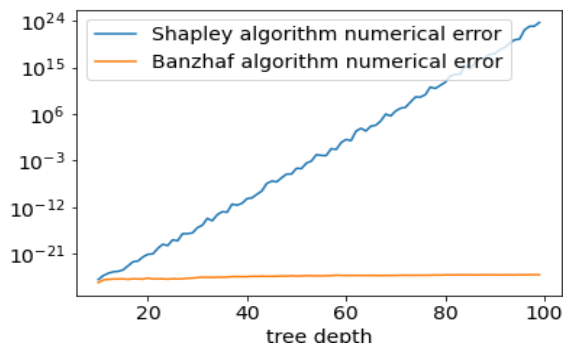


Figure 1: The numerical error for SYNTHETIC_SPARSE. One can see that if the tree depth is more than apx. 50, the error makes the current implementation of Shapley values unusable. Moreover, the error grows exponentially in the depth of the tree.

5.3 Numerical Accuracy

We observe that the algorithms for computing Shapley values – both our version (in both variants with complexities $O(TLD^2)$ and $O(TLD)$ resp.) and the original one (as implemented in the SHAP package [4]) – suffer numerical problems for large trees. To show that, we consider a simple artificial tree for which we know the answer for both Shapley values and Banzhaf values, namely the SYNTHETIC_SPARSE instance. We have observed that for trees of depth apx. 50 errors dominate completely the results, i.e., errors become apx. 1. In Figure 1 we visualise the numerical errors for Shapley values and Banzhaf values in the case of SYNTHETIC_SPARSE instance.

For more realistic settings we observe that numerical errors that can alter results even for smaller trees used in practice, e.g., there are differences in the ordering of the first 10 features for different Shapley-based implementations on the NHANES_GBDT dataset. Hence, usage of Shapley values in practice requires additional care to control these errors, as otherwise one is not guaranteed to obtain correct results.

5.4 Comparison of Global Impacts

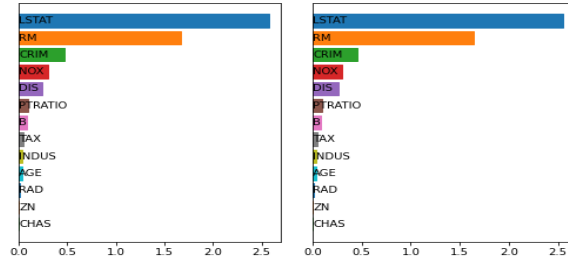
Now we present a comparison between `ban` and `shap_orig`. In Figures 2, 3, 4, 5, 6, 7, 8, and 9 we show the global impacts of features, as defined in the previous section. We confirm that the differences in this case are very small for small trees and visibly larger for large trees. However, one can observe differences for specific data points. In Table 1, we present the average Cayley distance between the feature orderings derived from the computed Shapley and Banzhaf values. In particular, when many features are used by the model, the difference in orderings becomes larger, as individual values become smaller.

5.5 Feature Values' Comparison

In order to pinpoint the reason why explanations for these models differ we have looked at specific instances. In particular, we present a detailed comparison of feature importances for individual predictions produced by the implemented algorithms. Figures 10, 11, 12, 13 show the MAE (Mean Average Error) and RMSE (Root Mean Square Error) between the respective Shapley and Banzhaf values for each individual feature through all the data points in the data sets BOSTON_GBDT, NHANES_GBDT, HEALTH_INSURANCE_GBDT, and FLIGHTS_GBDT. Formally, for each dataset \mathcal{D} out of those and each feature i used there, these are defined as:

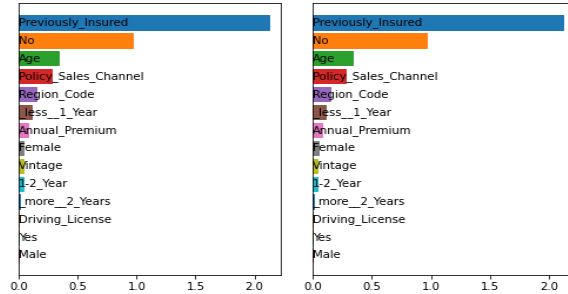
Ins/n	3	10	20
BOS_GBBDT	0.02	1.05	
NH_GBBDT	0.01	0.34	1.53
HI_GBBDT	0.02	0.73	
FL_GBBDT	0.23	3.08	8.63
BOS_DT	0.08	1.73	
NH_DT	0.33	4.33	11.62
HI_DT	1.10	6.79	
FL_DT	0.84	6.39	14.11

Table 1: The average modified Cayley distance for the n most important features for $n \in \{3, 10, 20\}$ between Shapley and Banzhaf values. The Cayley distance measures the number of swaps needed to switch from one permutation to another. In our modified version, we also support the case where the sets of considered most important features in the respective permutations are different. For a missing feature, we add it at the end of the permutation.



(a) Original Shapley values. (b) Banzhaf values.

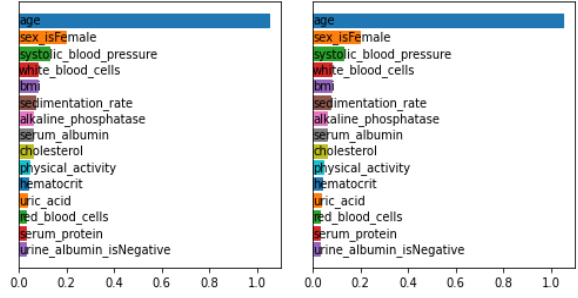
Figure 2: The global impacts of the individual features for the BOSTON_GBBDT dataset. We observe that the plots are indistinguishable.



(a) Original Shapley values. (b) Banzhaf values.

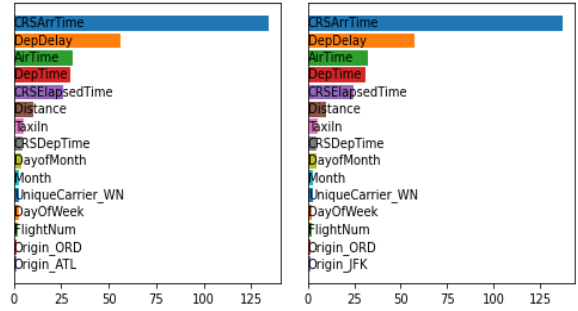
Figure 3: The features' global impacts for the HEALTH_INSURANCE_GBBDT dataset. We observe that the plots are indistinguishable.

$$\text{MAE}_i = \frac{1}{|\mathcal{D}|} \sum_{x \in \mathcal{D}} |\phi_i(x) - \beta_i(x)| \quad \text{RMSE}_i = \sqrt{\frac{1}{|\mathcal{D}|} \sum_{x \in \mathcal{D}} (\phi_i(x)^2 - \beta_i(x))^2}$$



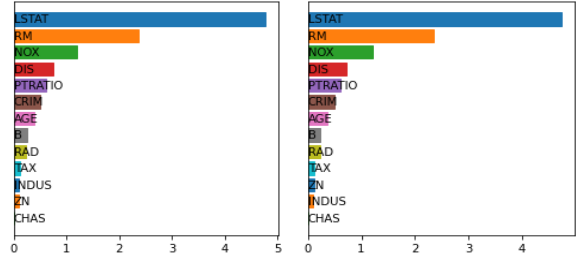
(a) Original Shapley value. (b) Banzhaf values.

Figure 4: The global impacts of the individual features for the NHANES_GBDT dataset. We observe that the plots are indistinguishable.



(a) Original Shapley value. (b) Banzhaf values.

Figure 5: The global impacts of the individual features for the FLIGHTS_GBDT dataset. We observe small differences in the ordering.

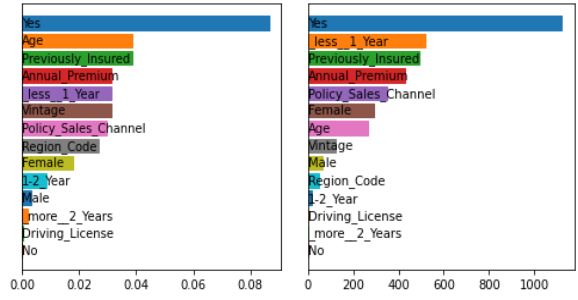


(a) Original Shapley values. (b) Banzhaf values.

Figure 6: The global impacts of the individual features for the BOSTON_DT dataset. We observe minor differences between plots.

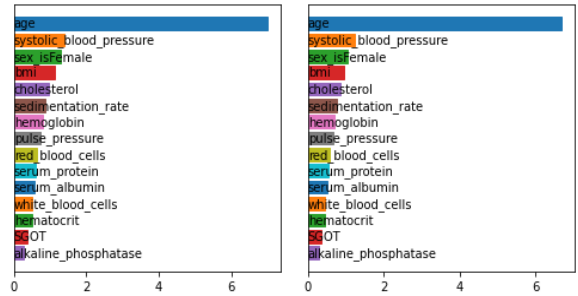
Above, $\phi_i(x)$ denotes the Shapley explanation of $f(x)$ for data point $x \in \mathcal{D}$, as computed by `shap_orig`. Similarly, $\beta_i(x)$ denotes the Banzhaf explanation of $f(x)$ for $x \in \mathcal{D}$ as computed by `ban`.

We observe that errors in Figures 10, 11, 12, 13 lie in the range of few small percent in relation to the possible ranges of global impacts. These errors indicate that when looking at specific data points one should expect only some differences in ordering of the features and only for features with similar scores. However,



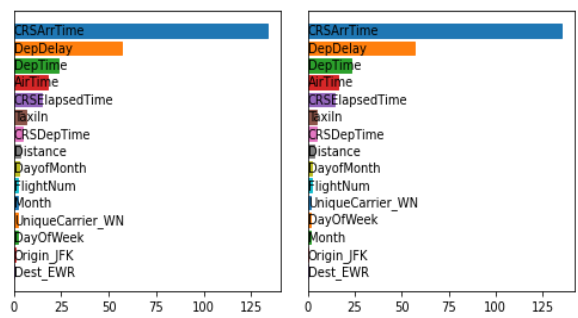
(a) Original Shapley values. (b) Banzhaf values.

Figure 7: The features' global impacts for the HEALTH_INSURANCE_DT dataset. We observe . We observe major differences between plots..



(a) Original Shapley value. (b) Banzhaf values.

Figure 8: The global impacts of the individual features for the NHANES_DT dataset. We observe that the plots are indistinguishable.



(a) Original Shapley value. (b) Banzhaf values.

Figure 9: The global impacts of the individual features for the FLIGHTS_DT dataset. We observe minor differences in the ordering.

this is the case only for the GBDT datasets, whereas when the DT algorithm is used these errors become dominating. As these plots do not seem to contain any valuable information, we have decided not to include them. This is further illustrated in the next figures which present scores for specific data-points.

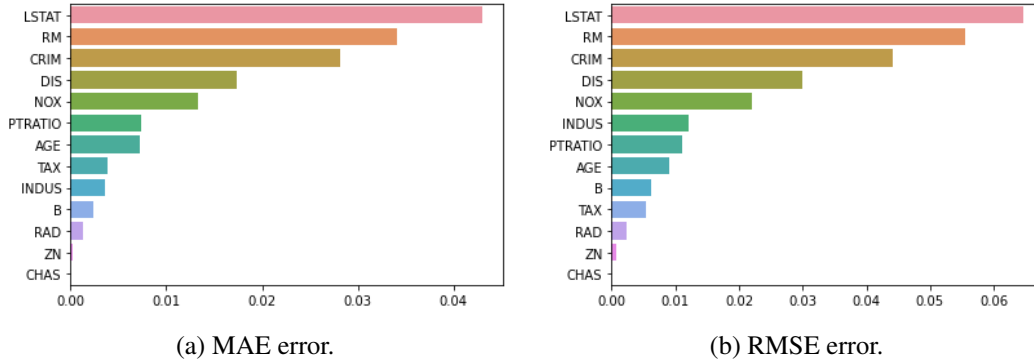


Figure 10: The MAE and RMSE error between Banzhaf and Shapley values for the BOSTON_GBDT dataset.

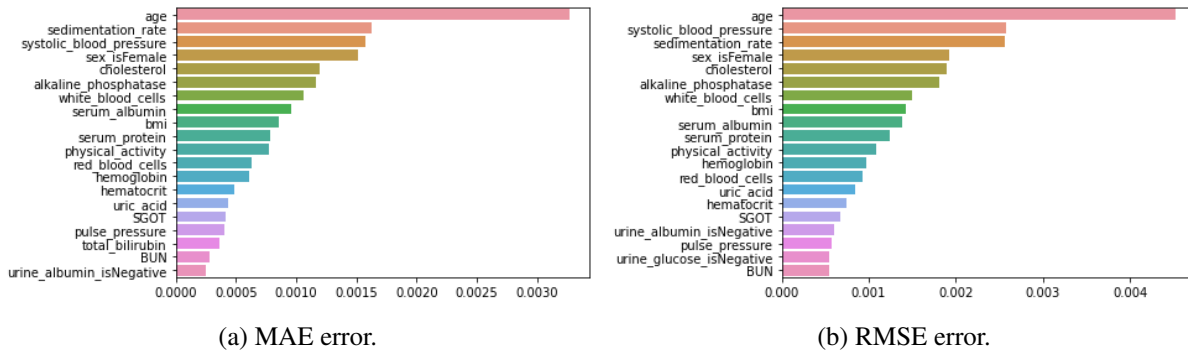


Figure 11: The MAE and RMSE error between Banzhaf and Shapley values for the NHANES_GBDT dataset.

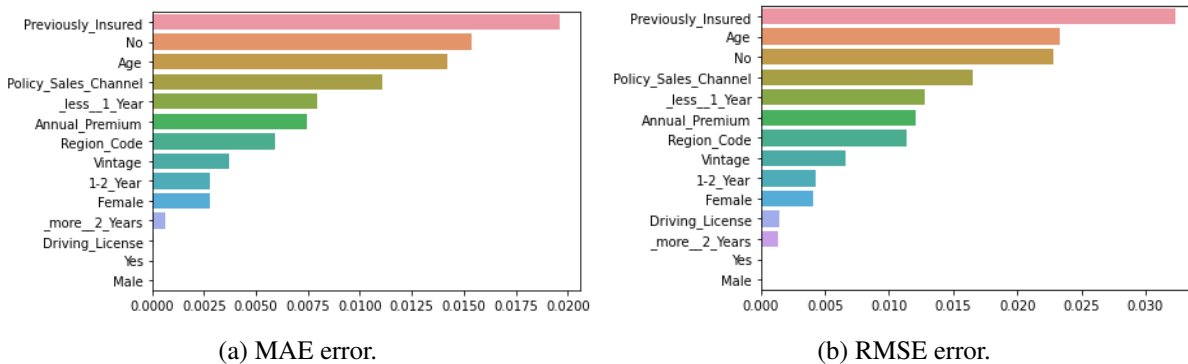


Figure 12: The MAE and RMSE error between Banzhaf and Shapley values for the HEALTH_INSURANCE_GBDT dataset.

In Figures 14, 15, 16, 17, 18, 19, 20, 21 we present “bad” examples for which the order of important features differs the most for Banzhaf and Shapley values for large trees. For small trees, differences do not change the overall interpretations, i.e., the ordering of the top features remains essentially the same, whereas for large trees we observe major differences in feature importance. In Figure 20, one can see larger differences in values, e.g., there is a difference in the most important value. These results seem to seemingly falsify Hypothesis 1. However, as we observed in Section 5.3 that numerical errors can be dominating in

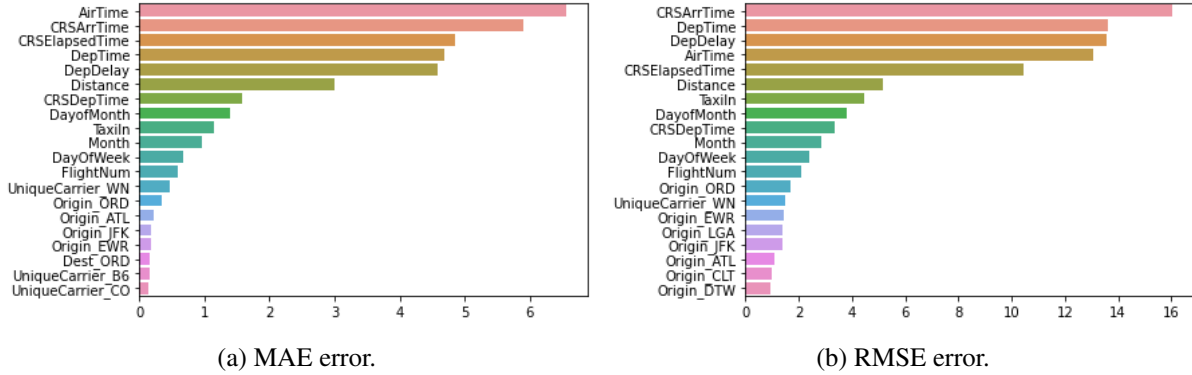


Figure 13: The MAE and RMSE error between Banzhaf and Shapley values for the FLIGHTS_GBDT dataset.

Shapley values computations. This is visualized on Figure 22 that visualizes differences between different implementations of Shapley values. Hence, the numerical errors can make specific Shapley explanations unusable for DT algorithms.

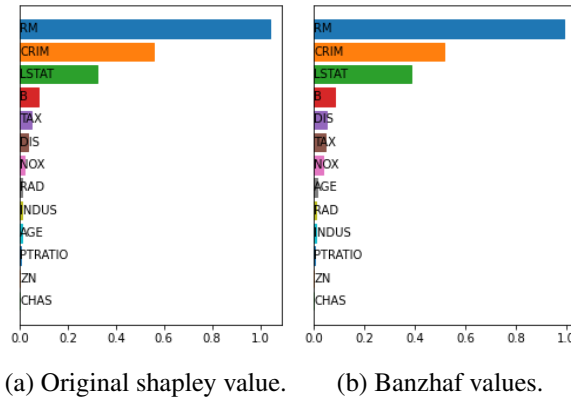
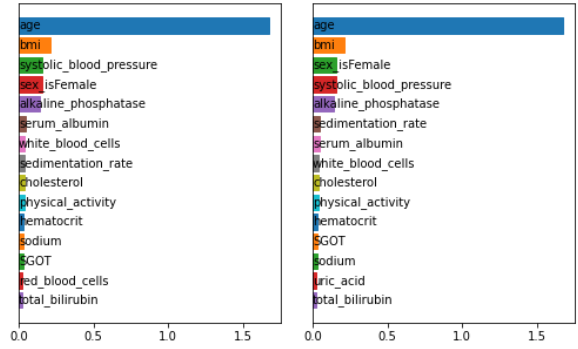


Figure 14: A “bad” example: Banzhaf and Shapley values for a data point for which they differ the most on the BOSTON_GBDT dataset.

5.6 Comparison of Running Times

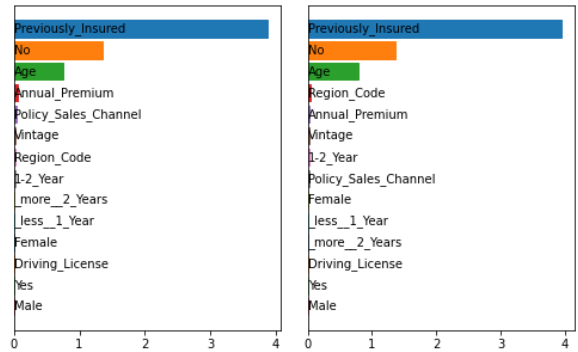
In this section, we compare the running times of the algorithms. In Table 2 we show the running times for different examples. It can be seen that ban is faster than all other methods, and using it can lead to considerable time savings for larger data-sets. For small depths, as used in these examples, shap_orig_a and shap_fast essentially run in the same time, whereas shap_orig is faster due to different implementation.

However, this changes with the increased depth of the trees as shown in Figure 23. We included our implementation of the original algorithm of Lundberg et al. (shap_orig_a) to avoid unfair comparison, e.g., differences in efficiency of data structures and preprocessing. We observe that the asymptotically faster (by a factor of D) versions of the algorithms for computing Shapley values and Banzhaf values are orders of magnitudes faster than the previous versions.



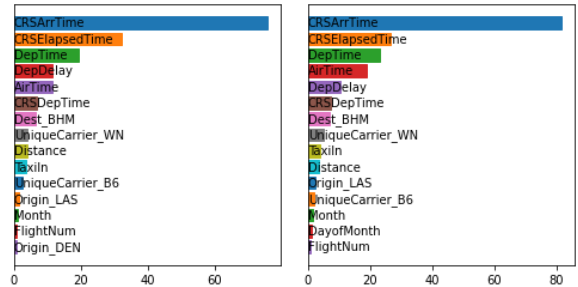
(a) Original shapley value. (b) Banzhaf values.

Figure 15: A “bad” example: Banzhaf and Shapley values for a data point for which they differ the most on the NHANES_GBDT dataset.



(a) Original shapley value. (b) Banzhaf values.

Figure 16: A “bad” example: Banzhaf and Shapley values for a data point for which they differ the most on the HEALTH_INSURANCE_GBDT dataset.



(a) Original shapley value. (b) Banzhaf values.

Figure 17: A “bad” example: Banzhaf and Shapley values for a data point for which they differ the most on the FLIGHTS_GBDT dataset.

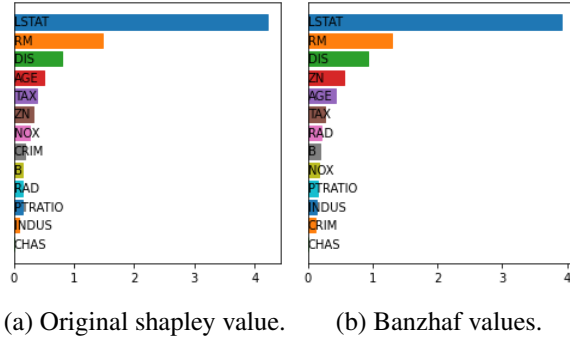


Figure 18: A “bad” example: Banzhaf and Shapley values for a data point for which they differ the most on the BOSTON_DT dataset.

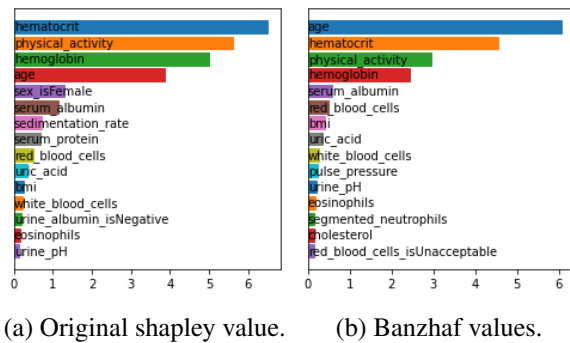


Figure 19: A “bad” example: Banzhaf and Shapley values for a data point for which they differ the most on the NHANES_DT dataset. We observe large differences caused by numerical errors.

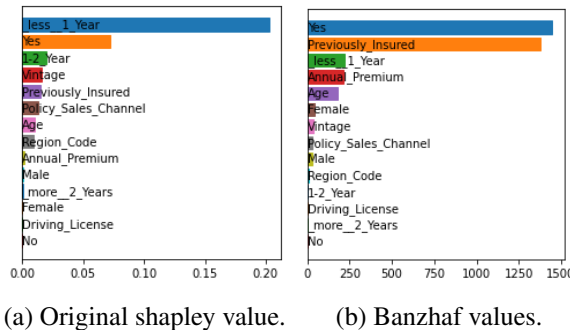


Figure 20: A “bad” example: Banzhaf and Shapley values for a data point for which they differ the most on the HEALTH_INSURANCE_DT dataset. We observe large differences caused by numerical errors.

5.7 Experimental Setup

All of the experiments were done using Intel(R) Xeon(R) CPU E5-2630 v4 @ 2.20GHz with 512 Gb of RAM using only one thread for computation. The operating system was Ubuntu 18.04.2 LTS. The binaries were compiled using clang version 6.0.0-1ubuntu2 with -O3 optimization.

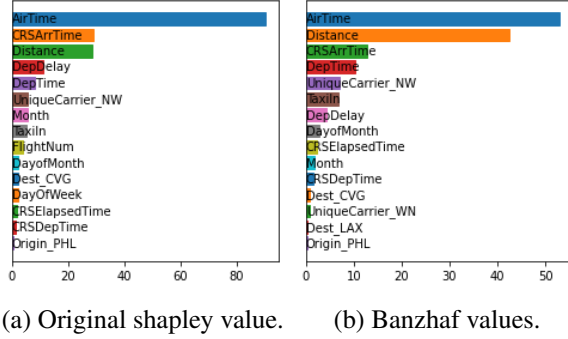


Figure 21: A “bad” example: Banzhaf and Shapley values for a data point for which they differ the most on the FLIGHTS_DT dataset. We observe large differences caused by numerical errors.

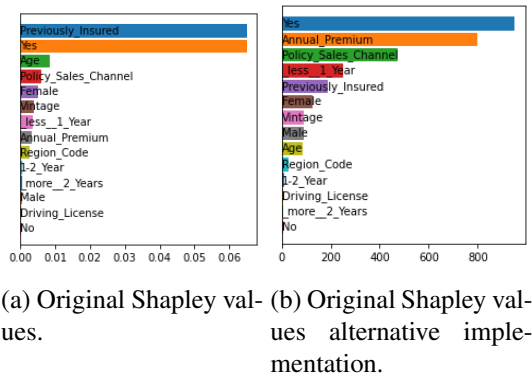


Figure 22: A “bad” example: comparing two implementations of Shapley values: `shap_orig` and `shap_orig_a` for a data point for which they differ the most on the HEALTH_INSURANCE_DT dataset. We observe large differences caused by numerical errors.

Ins	ban	shap_fast	shap_orig	shap_orig_a
BS_GBDT	0.48 s	0.56 s	0.63 s	0.70 s
HL_GBDT	23.63 s	51.73 s	1 m 9 s	35.32 s
NH_GBDT	50.20 s	2 m 28 s	2 m 56 s	1 m 28 s
FL_GBDT	13 m 18 s	1 h 47 m	1 h 50 m	48 m 8 s
BS_DT	0.41 s	0.42 s	0.41 s	0.42 s
NH_DT	3.57 s	34.92 s	42.87 s	45.58 s
HL_DT	4 m 55 s	23 m 18 s	30 m 55 s	35 m 3 s
FL_DT	14 m 28 s	5 h 23 m	5 h 9 m	5 h 40 m

Table 2: The comparison of running times for different algorithms. We observe that Banzhaf values implementation (ban) is substantially faster than all the Shapley value implementations on each instance.

6 The Basic Algorithm for Shapley and Banzhaf Values

In this section we describe in detail a variant of the $O(TLD^2 + n)$ time TREESHAP_PATH algorithm of Lundberg et al. [31]. We also show how it is adjusted to compute the Banzhaf values instead. Recall that

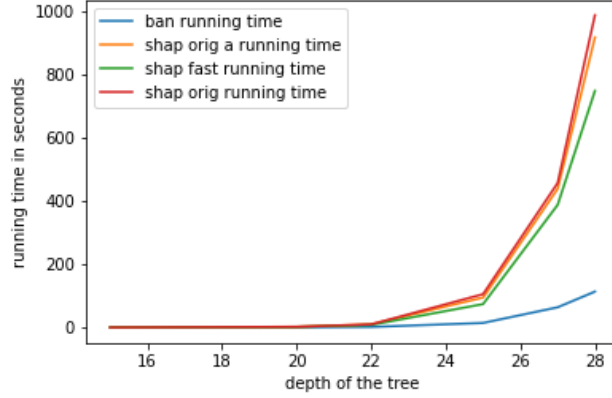


Figure 23: The comparison of running times for different tree sizes for the SYNTHETIC_DENSE instance.

T denotes the number of trees in the ensemble, and L and D bound the numbers of leaves and the depth of each of these trees, respectively. We first consider the case $T = 1$ (i.e., that the ensemble consists of a single tree \mathcal{T}) and then (in Section 6.4) we show how to handle larger tree ensembles.

For some non-root node v of the tree, denote by z_v the feature in the parent node p_v of v , i.e., $z_v = d_{p_v}$. Recall that F_v denotes the set of features in the ancestors of v , excluding the feature in v . So we have $F_\rho = \emptyset$ and $F_v = F_{p_v} \cup \{z_v\}$.

Recall that our ultimate goal is to compute for each $i \in U$:

1. Shapley values defined as:

$$\phi_i = \frac{1}{n} \sum_{S \subseteq U \setminus \{i\}} \binom{n-1}{|S|}^{-1} (g(S \cup \{i\}) - g(S)).$$

2. Banzhaf values defined as:

$$\beta_i = \frac{1}{2^{n-1}} \sum_{S \subseteq U \setminus \{i\}} (g(S \cup \{i\}) - g(S)).$$

where g is defined to be the output of Algorithm 1. We can also write:

$$g(S) := \sum_{l \in \mathcal{L}(\mathcal{T})} P[l, S] \cdot f(l), \quad (6)$$

where the values $P[\cdot, \cdot]$ are defined using Algorithm 1. More precisely, if Algorithm 1 is executed with subset $S \subseteq U$, then $P[v, S]$ for each $v \in \mathcal{T}$ equals the weight that the ancestor recursive calls assign to the subtree rooted at v . Formally, $P[\rho, S] = 1$, and for any $v \neq \rho$,

$$P[v, S] = \begin{cases} P[p_v, S] \cdot \frac{r_v}{r_{p_v}} & \text{if } z_v \notin S, \\ P[p_v, S] \cdot [x_{z_v} < t_{p_v}] & \text{if } z_v \in S, v = a_{p_v}, \\ P[p_v, S] \cdot [x_{z_v} \geq t_{p_v}] & \text{if } z_v \in S, v = b_{p_v}. \end{cases}$$

Denote by $I_{v,y}$ the minimal interval that x_y has to belong to in order to x end up being evaluated to a leaf in the subtree of v , i.e., so that $f(x) \in \{f(l) : l \in \mathcal{L}(\mathcal{T}[v])\}$. In particular, if no ancestor of v stores the feature y , we set $I_{v,y} = (-\infty, \infty)$. We say that $I_{v,y}$ is *non-trivial* if $I_{v,y} \neq I_{p_v,y}$. Observe that $I_{v,y}$ can only be non-trivial if $y = z_v$. Moreover, in that case we have

$$I_{v,y} = \begin{cases} I_{p_v,y} \cap (-\infty, t_{p_v}] & v = a_{p_v}, \\ I_{p_v,y} \cap (t_{p_v}, \infty) & v = b_{p_v}. \end{cases}$$

Hence, we obtain the following.

Observation 1. *All the non-trivial intervals $I_{v,y}$ for all possible $(v, y) \in \mathcal{T} \times U$, can be computed in $O(L)$ time.*

Let $y \in U$ be some feature. Denote by $c_v(y)$ the product of all the values r_u/r_{p_u} such that u is non-root (weak) ancestor of v and $z_u = y$. In particular, if $y \notin F_v$, then $c_v(y) = 1$. Similarly as was the case for the intervals $I_{v,y}$, a value $c_v(y)$ can only differ from $c_{p_v}(y)$ if $y = z_v$ (then we have $c_v(y) = c_{p_v}(y) \cdot r_v/r_{p_v}$). Hence, all such non-trivial values $c_v(y)$ can be computed in $O(L)$ time as well.

Let us start by describing the basic algorithm for Shapley values. To proceed, we introduce the following crucial notation. For any set $G \subseteq U$, let

$$\phi(v, G, k) := \frac{1}{|G| + 1} \sum_{\substack{S \subseteq G \\ |S|=k}} \binom{|G|}{k}^{-1} \cdot P[v, S]. \quad (7)$$

Roughly speaking, the values $\phi(v, G, k)$ can be computed using dynamic programming. Let us put

$$\phi(v, G) := \sum_{k=0}^{|G|} \phi(v, G, k).$$

6.1 Leaf Contributions

In this section we show that computing $\phi(l, F_l \setminus \{i\})$ for all pairs $l \in \mathcal{L}(\mathcal{T})$, $i \in F_l$ is sufficient to get all the sought Shapley values. In order to prove that, let us first observe some simple properties of the values $P[\cdot, \cdot]$.

Lemma 1. *Let $v \in \mathcal{T}$ and $Q \subseteq U$ and $y \in U \setminus Q$. Then:*

$$P[v, Q \cup \{y\}] = P[v, Q] \cdot \frac{[x_y \in I_{v,y}]}{c_v(y)}.$$

Proof. This can be proven by induction on the depth of v in \mathcal{T} . The claim holds obviously for $v = \rho$. So suppose v is non-root. First recall that if $z_v \neq y$, we have $[x_y \in I_{v,y}] = [x_y \in I_{p_v,y}]$ and $c_v(y) = c_{p_v}(y)$.

Suppose $z_v \notin Q \cup \{y\}$. Then:

$$\begin{aligned} P[v, Q \cup \{y\}] &= P[p_v, Q \cup \{y\}] \cdot \frac{r_v}{r_{p_v}} \\ &= P[p_v, Q] \cdot \frac{[x_y \in I_{v,y}]}{c_v(y)} \cdot \frac{r_v}{r_{p_v}} \\ &= P[v, Q] \cdot \frac{[x_y \in I_{v,y}]}{c_v(y)}. \end{aligned}$$

Otherwise, $z_v \in Q \cup \{y\}$. Assume wlog. $v = a_{p_v}$ – the case $v = b_{p_v}$ is symmetric. We have:

$$\begin{aligned} P[v, Q \cup \{y\}] &= P[p_v, Q \cup \{y\}] \cdot [x_{z_v} < t_{z_v}] \\ &= P[p_v, Q] \cdot \frac{[x_y \in I_{p_v, y}]}{c_{p_v}(y)} \cdot [x_{z_v} < t_{z_v}] \end{aligned}$$

If $z_v = y$, then $z_v \notin Q$ and we have $c_v(y) = c_{p_v}(y) \cdot \frac{r_v}{r_{p_v}}$ and $[x_y \in I_{v, y}] = [x_y \in I_{p_v, y}] \cdot [x_y < t_{z_v}]$. So in that case

$$\begin{aligned} P[v, Q \cup \{y\}] &= P[p_v, Q] \cdot \frac{[x_y \in I_{v, y}]}{c_v(y)} \cdot \frac{r_{p_v}}{r_v} \\ &= P[v, Q] \cdot \frac{[x_y \in I_{v, y}]}{c_v(y)} \end{aligned}$$

If on the other hand we have $y \neq z_v \in Q$, then:

$$P[v, Q \cup \{y\}] = P[p_v, Q] \cdot \frac{[x_y \in I_{v, y}]}{c_v(y)} \cdot [x_{z_v} < t_{z_v}] = P[v, Q] \cdot \frac{[x_y \in I_{v, y}]}{c_v(y)}.$$

□

Lemma 2. *Let $v \in \mathcal{T}$ be non-root and $Q \subseteq U \setminus \{z_v\}$. Then*

$$P[v, Q] = P[p_v, Q] \cdot \frac{c_v(z_v)}{c_{p_v}(z_v)}.$$

Proof. It is enough to note that $\frac{c_v(z_v)}{c_{p_v}(z_v)} = \frac{r_v}{r_{p_v}}$. □

The following lemma, which we prove later on, states an intuitive fact that $\phi(v, G)$ does not depend on the features in G that do not appear in the ancestors of v .

Lemma 3. *Let $v \in \mathcal{T}$ and $G \subseteq U$. Suppose $y \in U \setminus G \setminus F_v$. Then:*

$$\phi(v, G \cup \{y\}) = \phi(v, G).$$

Let us now expand the sum (1) using (6) to pinpoint the individual contributions of each leaf l into ϕ_i .

$$\begin{aligned} \phi_i &= \frac{1}{n} \sum_{S \subseteq U \setminus \{i\}} \binom{n-1}{|S|}^{-1} (g(S \cup \{i\}) - g(S)) \\ &= \frac{1}{n} \sum_{S \subseteq U \setminus \{i\}} \binom{n-1}{|S|}^{-1} \left(\sum_{l \in \mathcal{L}(\mathcal{T})} f(l) (P[l, S \cup \{i\}] - P[l, S]) \right) \end{aligned}$$

By subsequently applying Lemma 1, changing the summation order, using (6), and finally applying Lemma 3, we get:

$$\begin{aligned}
\phi_i &= \frac{1}{n} \sum_{S \subseteq U \setminus \{i\}} \binom{n-1}{|S|}^{-1} \left(\sum_{l \in \mathcal{L}(\mathcal{T})} f(l) \cdot P[l, S] \left(\frac{[x_i \in I_{l,i}]}{c_l(i)} - 1 \right) \right) \\
&= \sum_{l \in \mathcal{L}(\mathcal{T})} f(l) \cdot \left(\frac{[x_i \in I_{l,i}]}{c_l(i)} - 1 \right) \left(\frac{1}{n} \sum_{S \subseteq U \setminus \{i\}} \binom{n-1}{|S|}^{-1} P[l, S] \right) \\
&= \sum_{l \in \mathcal{L}(\mathcal{T})} f(l) \cdot \left(\frac{[x_i \in I_{l,i}]}{c_l(i)} - 1 \right) \cdot \phi(l, U \setminus \{i\})
\end{aligned}$$

Since $\left(\frac{[x_i \in I_{l,i}]}{c_l(i)} - 1 \right) = 0$ when $i \notin F_l$, we actually have:

$$\phi_i = \sum_{\substack{l \in \mathcal{L}(\mathcal{T}) \\ i \in F_l}} f(l) \cdot \left(\frac{[x_i \in I_{l,i}]}{c_l(i)} - 1 \right) \cdot \phi(l, F_l \setminus \{i\}). \quad (8)$$

So indeed, Equation (8) provides an $O(LD)$ -time reduction of the problem of computing Shapley values to computing the values $\phi(l, F_l \setminus \{i\})$ for all $l \in \mathcal{L}(\mathcal{T})$ and $i \in F_l$.

6.2 Dynamic Programming

In this section we show how the values $\phi(v, G, k)$ can be computed recursively to avoid iterating through all subsets in the sum (7). For convenience let us define $\phi(v, G, k) = 0$ for $k < 0$ or $k > |G|$.

Lemma 4. *Let $v \in \mathcal{T}$, $G \subseteq U$ and $k \in \{0, \dots, |G|\}$. Let $y \in U \setminus G$. Then:*

$$\phi(v, G \cup \{y\}, k) = \frac{|G| + 1 - k}{|G| + 2} \cdot \phi(v, G, k) + \frac{k}{|G| + 2} \cdot \frac{[x_y \in I_{v,y}]}{c_v(y)} \cdot \phi(v, G, k - 1).$$

Proof. Let $m = |G| + 1$ and $X = \phi(v, G \cup \{y\}, k)$. By Lemma 1 we get:

$$\begin{aligned}
X &= \sum_{\substack{S \subseteq G \cup \{y\} \\ |S|=k}} \frac{1}{m+1} \binom{m}{k}^{-1} P[v, S] \\
&= \sum_{\substack{S \subseteq G \\ |S|=k}} \frac{1}{m+1} \binom{m}{k}^{-1} P[v, S] + \sum_{\substack{y \in S \subseteq G \cup \{y\} \\ |S|=k}} \frac{1}{m+1} \binom{m}{k}^{-1} P[v, S] \\
&= \sum_{\substack{S \subseteq G \\ |S|=k}} \frac{m-k}{m+1} \cdot \frac{1}{m} \binom{m-1}{k}^{-1} P[v, S] + \sum_{\substack{S \subseteq G \\ |S|=k-1}} \frac{k}{m+1} \cdot \frac{[x_y \in I_{v,y}]}{c_v(y)} \cdot \frac{1}{m} \binom{m-1}{k-1}^{-1} P[v, S] \\
&= \frac{m-k}{m+1} \cdot \phi(v, G, k) + \frac{k}{m+1} \cdot \frac{[x_y \in I_{v,y}]}{c_v(y)} \cdot \phi(v, G, k-1). \quad \square
\end{aligned}$$

Now, given the recursive formula of Lemma 4, we are ready to prove Lemma 3.

Proof of Lemma 3. Recall that $y \in U \setminus G \setminus F_v$ and thus $\frac{[x_y \in I_{v,y}]}{c_v(y)} = 1$. By Lemma 4, we have:

$$\begin{aligned}
\phi(v, G \cup \{y\}) &= \sum_{k=0}^{|G|+1} \phi(v, G \cup \{y\}, k) \\
&= \sum_{k=0}^{|G|+1} \frac{|G|+1-k}{|G|+2} \cdot \phi(v, G, k) + \sum_{k=0}^{|G|+1} \frac{k}{|G|+2} \cdot \phi(v, G, k-1) \\
&= \sum_{k=0}^{|G|} \frac{|G|+1-k}{|G|+2} \cdot \phi(v, G, k) + \sum_{k=0}^{|G|} \frac{k+1}{|G|+2} \cdot \phi(v, G, k) \\
&= \sum_{k=0}^{|G|} \phi(v, G, k) \\
&= \phi(v, G).
\end{aligned}$$

□

By Lemma 4, we can compute all the values of the form $\phi(v, G, \cdot)$ in $O(|G|)$ time given:

- either the values $\phi(v, G \setminus \{y^-\}, \cdot)$ for any $y^- \in G$,
- or the values $\phi(v, G \cup \{y^+\}, \cdot)$ for any $y^+ \in U \setminus G$.

To describe our basic algorithm, we need one more simple observation.

Lemma 5. *Let $v \in \mathcal{T}$ be a non-root node and let $Q \subseteq U \setminus \{z_v\}$. Then, for all k ,*

$$\phi(v, Q, k) = \phi(p_v, Q, k) \cdot \frac{c_v(z_v)}{c_{p_v}(z_v)}.$$

Proof. By Lemma 2, the sum (7) defining $\phi(v, Q, k)$ can be obtained by multiplying every term in the sum defining $\phi(p_v, Q, k)$ by $\frac{c_v(z_v)}{c_{p_v}(z_v)}$. □

Now we are ready to describe the basic algorithm. The algorithm will maintain a real vector Ψ :

$$\Psi(v, G) = (\Psi_k)_{k=0}^{|G|} = (\phi(v, G, k))_{k=0}^{|G|}$$

for some $v \in \mathcal{T}$ and $G \subseteq U$. We call this vector Ψ a *state*. Note that $\|\Psi\|_1 = \phi(v, G)$. The algorithms will perform a number of operations on the state.

We will need the two following vector functions $\text{AddFeature}(\mathbf{b}, \delta) : \mathbb{R}^\ell \times \mathbb{R} \rightarrow \mathbb{R}^{\ell+1}$ and $\text{DelFeature}(\mathbf{b}, \delta) : \mathbb{R}^\ell \times \mathbb{R} \rightarrow \mathbb{R}^{\ell-1}$. Let us assume $\mathbf{b} := (b_k)_{k=1}^\ell$ and for convenience put $b_{-1} = b_{\ell+1} = 0$. Then AddFeature is defined:

$$(\text{AddFeature}(\mathbf{b}, \delta))_k = \frac{\ell+1-k}{\ell+2} \cdot b_k + \frac{k}{\ell+2} \cdot \delta \cdot b_{k-1}.$$

The function DelFeature is a reverse of AddFeature . Formally, if $b'_{-1} = 0$ and $(\text{DelFeature}(\mathbf{b}, \delta))_k = b'_k$, then:

$$b'_k = \frac{\ell+1}{\ell} \left(b_k - \frac{k}{\ell+1} \cdot \delta \cdot b'_{k-1} \right).$$

Algorithm 2 Computing values $\phi_i, i \in U$, in $O(LD^2)$ time.

procedure $\text{Traverse}(v)$

```

1: if  $z_v \in F_{p_v}$  then
2:    $\Psi := \text{DelFeature}(\Psi, \delta_{v,z_v})$ 
3:    $\Psi := \Psi \cdot \frac{c_v(z_v)}{c_{p_v}(z_v)}$ 
4:    $\Psi := \text{AddFeature}(\Psi, \delta_{v,z_v})$ 
5: if  $v \notin \mathcal{L}(\mathcal{T})$  then
6:    $\text{Traverse}(a_v)$ 
7:    $\text{Traverse}(b_v)$ 
8: else
9:   for  $i \in F_v$  do
10:     $\Psi := \text{DelFeature}(\Psi, \delta_{v,i})$ 
11:     $\phi_i := \phi_i + \|\Psi\|_1 \cdot f(v) \cdot (\delta_{v,i} - 1)$ 
12:     $\Psi := \text{AddFeature}(\Psi, \delta_{v,i})$ 
13:    $\Psi := \text{DelFeature}(\Psi, \delta_{v,z_v})$ 
14:    $\Psi := \Psi \cdot \frac{c_{p_v}(z_v)}{c_v(z_v)}$ 
15: if  $z_v \in F_{p_v}$  then
16:    $\Psi := \text{AddFeature}(\Psi, \delta_{v,z_v})$ 

```

function TreeSHAP

```

1:  $\phi = (0, 0, \dots, 0) \in \mathbb{R}^n$ 
2:  $\Psi := 0$ 
3:  $\text{Traverse}(a_\rho)$ 
4:  $\text{Traverse}(b_\rho)$ 
5: return  $\phi$ 

```

Intuitively, the purpose of the functions AddFeature and DelFeature is to apply the dynamic programming transition of Lemma 4. Defining these functions in such a general way will prove very useful in the implementation of a faster algorithm (Section 7). Clearly, both functions can be implemented in $O(\ell)$ time.

The goal of a recursive procedure $\text{Traverse}(v)$ (see Algorithm 2) is to iterate through all the states $\Psi(v, F_v), v \in \mathcal{T}[v]$. At a leaf $l \in \mathcal{L}(\mathcal{T})$, the contributions of the leaf l to each relevant ϕ_i will be calculated. Let us introduce one more notation (also used in the pseudocode of Traverse):

$$\delta_{v,y} := \frac{[x_v \in I_{v,y}]}{c_v(y)}. \quad (9)$$

More precisely, when $\text{Traverse}(v)$ is called, we guarantee that the current state is $\Psi(p_v, F_{p_v})$. In particular, for $p_v = \rho$, $\Psi = (\phi(\rho, \emptyset, 0)) = (0)$. The first step is to move the state to $\Psi(v, F_v)$. This is done in three substeps:

1. First, if $z_v \in F_{p_v}$, we perform

$$\Psi := \text{DelFeature}(\Psi, \delta_{v,z_v}).$$

Then, by Lemma 4, the state equals $\Psi(p_v, F_{p_v} \setminus \{z_v\})$.

2. Next, we perform

$$\Psi := \Psi \cdot \frac{c_v(z_v)}{c_{p_v}(z_v)}.$$

Afterwards, since $z_v \notin F_{p_v} \setminus z_v$, by Lemma 5, the state equals $\Psi(v, F_{p_v} \setminus \{z_v\})$.

3. Then, we perform

$$\Psi := \text{AddFeature}(\Psi, \delta_{v, z_v}).$$

which, again by Lemma 4, moves the state to $\Psi(v, F_v)$.

If v is non-leaf, $\text{Traverse}(a_v)$ and $\text{Traverse}(b_v)$ are called recursively to process the subtrees of v . Note that the required state invariant is satisfied at the beginning of these calls. After the recursive calls return, we move the state back to $\Psi(p_v, F_{p_v})$ by reversing the steps 1-3.

If v is a leaf, for each $i \in F_v$ we do the following:

1. We move the state to $\Psi(v, F_v \setminus \{i\})$ by performing $\Psi := \text{DelFeature}(\Psi, \delta_{v, i})$.
2. We compute $\|\Psi\|_1$ to obtain $\phi(v, F_v \setminus \{i\})$ and add the contribution $\phi(v, F_v \setminus \{i\}) \cdot f(v) \cdot \left(\frac{[x_i \in I_{v, i}]}{c_v(i)} - 1 \right)$ to ϕ_i .
3. We move the state back to $\Psi(v, F_v)$ by running $\Psi := \text{AddFeature}(\Psi, \delta_{v, i})$.

Clearly, the computation at each non-leaf node $v \in \mathcal{T}$ costs $O(|F_v|) = O(D)$ time. On the other hand, for a leaf node l , we spend $O(|F_l|^2) = O(D^2)$ time. As a result, the total running time of the algorithm is $O(LD^2)$.

For clarity of the pseudocode, we assume that $\delta_{v, i}$ for any $i \in U$ can be computed in $O(1)$ time while inside the call $\text{Traverse}(v)$. We now justify this assumption. In the beginning of Section 6 we argued how the values $I_{v, y}$ and $c_v(y)$, $y \in U$, can differ from the corresponding values $I_{p_v, y}$ and $c_{p_v}(y)$ only for a single $y = z_v$. Note that the call $\text{Traverse}(v)$ only requires values of the form $I_{v, \cdot}$, $c_v(\cdot)$. As a result, both these sets of values can be maintained using global arrays $\mathbf{I} : U \rightarrow \mathbb{R}^2$ and $\mathbf{c} : U \rightarrow \mathbb{R}$. When the call $\text{Traverse}(v)$ starts, we only need to update $\mathbf{I}[z_v]$ and $\mathbf{c}[z_v]$ to reflect the difference between the $I_{v, \cdot}, c_v(\cdot)$ and $I_{p_v, \cdot}, c_{p_v}(\cdot)$. When the call ends, we revert that change to the arrays \mathbf{I}, \mathbf{c} .

6.3 Banzhaf Values

The same Algorithm 2 can be used to compute Banzhaf values. We only need to change the definition of a state $\Psi(v, G)$.

Instead of values $\phi(v, G, k)$, we base our dynamic programming computation on values $\beta(v, G)$ defined as follows.

$$\beta(v, G) := \frac{1}{2^{|G|}} \sum_{S \subseteq G} y(v, G). \quad (10)$$

The third coordinate is dropped since the coefficient of the summands in (10) do not depend on the size of the set S . We now show an analogue of Lemma 4 for Banzhaf values.

Lemma 6. *Let $v \in \mathcal{T}$ and $G \subseteq U$. Let $y \in U \setminus G$. Then:*

$$\beta(v, G \cup \{y\}) = \frac{1}{2} \left(1 + \frac{[x_y \in I_{v, y}]}{c_v(y)} \right) \beta(v, G).$$

Proof. Let $m = |G|$. By Lemma 1 we have:

$$\begin{aligned}
\beta(v, G \cup \{y\}) &= \sum_{S \subseteq G \cup \{y\}} \frac{1}{2^{m+1}} P[v, S] \\
&= \sum_{S \subseteq G} \frac{1}{2^{m+1}} P[v, S] + \sum_{y \in S \subseteq G \cup \{y\}} \frac{1}{2^{m+1}} P[v, S] \\
&= \sum_{S \subseteq G} \frac{1}{2} \cdot \frac{1}{2^m} P[v, S] + \sum_{S \subseteq G} \frac{1}{2} \cdot \frac{[x_y \in I_{v,y}]}{c_v(y)} \cdot \frac{1}{2^m} P[v, S] \\
&= \frac{1}{2} \left(1 + \frac{[x_y \in I_{v,y}]}{c_v(y)} \right) \beta(v, G). \quad \square
\end{aligned}$$

By Lemma 6, it also follows that for $y \notin F_v$, we have $\beta(v, G \cup \{y\}) = \beta(v, G)$, which gives a Banzhaf analogue of Lemma 3. Similarly, the proof of Lemma 5 carries on to Banzhaf values and we get that for $z_v \notin Q$ we have

$$\beta(v, Q) = \beta(p_v, Q) \cdot \frac{c_v(z_v)}{c_{p_v}(z_v)}.$$

Finally, we can analogously extract the individual leaf contributions to the Banzhaf values and get exactly the same formula:

$$\beta_i = \sum_{\substack{l \in \mathcal{L}(\mathcal{T}) \\ i \in F_l}} f(l) \cdot \left(\frac{[x_i \in I_{l,i}]}{c_l(i)} - 1 \right) \cdot \beta(l, F_l \setminus \{i\}).$$

The above discussion shows that precisely the same Algorithm 2 can be used if we modify the procedures `AddFeature`, `DelFeature` to operate on the Banzhaf state $\Psi(v, G) := \beta(v, G)$ in place of the Shapley state, i.e., to work according to Lemma 6 instead of Lemma 4. Observe that the implementation of these operations is simpler for Banzhaf values and all can be implemented in constant time.

Therefore, computing all values $\beta(l, F_l)$ for $l \in \mathcal{L}(\mathcal{T})$ takes only $O(L)$ time. Computing all the values $\beta(l, F_l \setminus \{i\})$ (and thus individual leaf contributions) for $l \in \mathcal{L}(\mathcal{T})$ and $i \in F_l$, however, still takes $O(LD)$ time since even the number of such pairs (l, i) can be $\Theta(LD)$. Nevertheless, this is already a factor- D speed-up over the basic algorithm for computing Shapley values.

6.4 Handling Multiple Trees

If the tree ensemble consists of more than one tree, i.e., $T > 1$, the output of the model is taken to be the average of the outputs of the individual trees. Since so far $g(S)$ was meant to approximate $\mathbb{E}[f(x_S, X_{\bar{S}})]$ for a single tree, by linearity of expectations, we can redefine $g(S)$ to be the average $g(S)$ over the individual trees.

In the implementation, all we need to do is to run Algorithm 2 for each of the individual trees, but we have to initialize $\phi = (0, \dots, 0) \in \mathbb{R}^n$ only once; we should not do it for each individual tree. After we are finished, the values ϕ_i should be divided by T . Note that, since the $O(n)$ term in the $O(LD^2 + n)$ bound came only from initializing the vector ϕ , the running time for T trees is $O(TLD^2 + n)$.

7 Faster Algorithm for Tree Ensembles

Recall Equation (8) that reduced the computation of all ϕ_i to computing individual $O(LD)$ leaf contributions

$$\left(\frac{[x_i \in I_{l,i}]}{c_l(i)} - 1 \right) \cdot f(l) \cdot \phi(l, F_l \setminus \{i\})$$

Let \mathcal{L}_v denote the set of leaves $l \in \mathcal{T}[v]$ such that v is the nearest ancestor w of l with $z_w = z_v$. Note that \mathcal{L}_v might not contain all the leaves in $\mathcal{T}[v]$ if some descendant of v satisfies $z_w = z_v$. What is important, for all $l \in \mathcal{L}_v$ we have

$$\left(\frac{[x_{z_v} \in I_{l,z_v}]}{c_l(z_v)} - 1 \right) = \left(\frac{[x_{z_v} \in I_{v,z_v}]}{c_v(z_v)} - 1 \right).$$

Moreover, note that the sets $\{\mathcal{L}_v : v \in \mathcal{T}, z_v = i\}$ form a partition of the set $\{l \in \mathcal{L}(\mathcal{T}) : i \in F_l\}$. Let us also set:

$$\Phi^-(v) := \sum_{l \in \mathcal{L}_v} f(l) \cdot \phi(l, F_l \setminus \{z_v\}).$$

Therefore, we can rewrite (8) as follows:

$$\begin{aligned} \phi_i &= \sum_{\substack{l \in \mathcal{L}(\mathcal{T}) \\ i \in F_l}} f(l) \cdot \left(\frac{[x_i \in I_{l,i}]}{c_l(i)} - 1 \right) \cdot \phi(l, F_l \setminus \{i\}) \\ &= \sum_{\substack{v \in \mathcal{T} \\ z_v = i}} \sum_{l \in \mathcal{L}_v} f(l) \cdot \left(\frac{[x_i \in I_{l,i}]}{c_l(i)} - 1 \right) \cdot \phi(l, F_l \setminus \{i\}) \\ &= \sum_{\substack{v \in \mathcal{T} \\ z_v = i}} \left(\frac{[x_i \in I_{v,i}]}{c_v(i)} - 1 \right) \sum_{l \in \mathcal{L}_v} f(l) \cdot \phi(l, F_l \setminus \{i\}) \\ &= \sum_{\substack{v \in \mathcal{T} \\ z_v = i}} \left(\frac{[x_i \in I_{v,i}]}{c_v(i)} - 1 \right) \cdot \Phi^-(v). \end{aligned}$$

Note that the above derivation provides an $O(L)$ -time reduction of computing all ϕ_i to computing all values $\Phi^-(v)$. The remaining part of this section is thus devoted to computing the values $\Phi^-(v)$, $v \in \mathcal{T}$.

Before we continue, we need to make a subtle change to our previous algorithm. Both the correctness and efficiency of our algorithm will crucially rely on the assumption that all sets F_l for $l \in \mathcal{L}(\mathcal{T})$ have the same size. This could be ensured, for example, by extending all smaller F_l with $D - |F_l|$ distinct dummy features that do not appear in F_l – recall that, by Lemma 3, adding dummy features does not change $\phi(v, G)$, for any $G \subseteq U$, so it does not influence our results. Unfortunately, adding a dummy feature to F_l by simply using Lemma 4 costs $\Theta(D)$ time. Therefore, if T was very unbalanced, padding all F_l could cost as much as $\Theta(LD^2)$ time.

Instead, let q_1, \dots, q_D be distinct artificial features *not* appearing in the nodes of \mathcal{T} . For *all* $v \in \mathcal{T}$ let us define

$$F_v^* = F_v \cup \{q_1, \dots, q_{D-|F_v|}\}.$$

Observe that then $F_\rho^* = \{q_1, \dots, q_D\}$ for the root ρ of \mathcal{T} , and for each non-root v we have

$$F_v^* = \begin{cases} F_{p_v}^* & \text{if } z_v \in F_{p_v} \\ F_{p_v}^* \setminus \{q_{D-|F_{p_v}|}\} \cup \{z_v\} & \text{otherwise.} \end{cases}$$

With sets F_v^* defined like this, $v \in \mathcal{T}$, by Lemma 3, we have:

$$\phi(v, F_v) = \phi(v, F_v^*),$$

and consequently:

$$\Phi^-(v) = \sum_{l \in \mathcal{L}_v} f(l) \cdot \phi(l, F_l^* \setminus \{z_v\}).$$

We modify the basic algorithm computing all the states $\Psi(v, F_v)$ so that it computes all the states $\Psi(v, F_v^*)$. It is very easy to change it to achieve that. First of all, the initial state $\Psi(\rho, F_\rho^*)$ is initialized in $O(D^2) = O(LD)$ time by applying Lemma 4 D times. Recall that the first step of `Traverse` is to perform $\Psi := \text{DelFeature}(\Psi, \delta_{v, z_v})$ if $z_v \in F_{p_v}$. Now, all we need to do is to add an extra condition that, if $z_v \notin F_{p_v}$, we also perform $\Psi := \text{DelFeature}(\Psi, \delta_{v, q_{D-|F_{p_v}|}})$ to “remove” a dummy feature from the state. Of course, this change has to be reflected also in the code that undoes state manipulation after the recursive calls return. See Algorithm 3.

The faster algorithm (implemented using a recursive procedure `TraverseFast`) avoids computing, for each $l \in \mathcal{L}(\mathcal{T})$, the states $\Psi(l, F_l^* \setminus \{i\})$ for all $i \in F_l$, which could take as much as $\Theta(LD^2)$ time in the basic algorithm. However, to achieve speed-up, the faster algorithm uses additional “bottom-up” steps (i.e., following the recursive calls). These steps compute some auxiliary data that we describe next.

For all $v \in \mathcal{T}$, let us define vectors $\Gamma(v), S(v) \in \mathbb{R}^D$, such that for $k = 0, \dots, D$:

$$\begin{aligned} \Gamma(v)_k &= \sum_{l \in \mathcal{L}_v} f(l) \cdot \phi(l, F_l^*, k), \\ S(v)_k &= \sum_{l \in \mathcal{L}(\mathcal{T}[v])} f(l) \cdot \phi(l, F_l^*, k). \end{aligned}$$

Lemma 7. *The vectors $S(v)$ and $\Gamma(v)$ for all $v \in \mathcal{T}$ and $k \in \{0, \dots, D\}$ can be computed using additional bottom-up steps in `TraverseFast` that cost $O(LD)$ extra time in total.*

Proof. First note that for $l \in \mathcal{L}(\mathcal{T})$ we have $S(v, k) = f(l) \cdot \phi(l, F_l^*, k)$ and $\phi(l, F_l^*, k) \in \Psi(l, F_l^*)$ which is a state that the basic procedure `Traverse` computes.

For all non-leaf nodes $v \in \mathcal{T}$ we in turn have

$$S(v) = S(a_v) + S(b_v),$$

and thus each of such $O(LD)$ values $S(v)_k$ can be computed in constant time after the recursive calls return.

Given the values $S(v)_k$, it is not very hard to obtain values $\Gamma(v)_k$. Let Q_v be the set of nodes $w \in \mathcal{T}[v]$ such that $z_w = z_v$ and v is the nearest ancestor of w satisfying $z_w = z_v$. Note that we have

$$\mathcal{L}_v = \mathcal{L}(\mathcal{T}[v]) \setminus \left(\bigcup_{w \in Q_v} \mathcal{L}(\mathcal{T}[w]) \right),$$

and thus

$$\Gamma(v) = S(v) - \sum_{w \in Q_v} S(w).$$

Observe that the total size of sets Q_v (over all $v \in \mathcal{T}$) is $O(L)$, so if we are allowed to iterate through Q_v whenever we wish to compute $\Gamma(v)$, the computation of $\Gamma(v)$ takes $O(LD)$ time as well. Let $g_{w,j}$ denote

Algorithm 3 Computing values $\phi_i, i \in U$, in $O(LD)$ time.

```

procedure TraverseFast( $v$ )
1: if  $z_v \in F_{p_v}$  then
2:    $\Psi := \text{DelFeature}(\Psi, \delta_{v,z_v})$ .
3:    $\text{Push}(H[z_v], v)$ .
4: else
5:    $\Psi := \text{DelFeature}(\Psi, \delta_{v,q_{D-|F_{p_v}|}})$ .
6:  $\Psi := \Psi \cdot \frac{c_v(z_v)}{c_{p_v}(z_v)}$ .
7:  $\Psi := \text{AddFeature}(\Psi, \delta_{v,z_v})$ .
8: if  $v \notin \mathcal{L}(\mathcal{T})$  then
9:    $\text{TraverseFast}(a_v)$ .
10:   $\text{TraverseFast}(b_v)$ .
11:   $S(v) := S(a_v) + S(b_v)$ .
12: else
13:   $S(v) := f(v) \cdot \Psi$ .
14:  $\Gamma(v) := S(v)$ 
15: while  $\text{Top}(H[z_v]) \neq v$  do
16:   $w := \text{Pop}(H[z_v])$ 
17:   $\Gamma(v) := \Gamma(v) - S(w)$ 
18:  $\Gamma^-(v) := \text{DelFeature}(\Gamma(v), \delta_{v,z_v})$ .
19:  $\phi_i := \phi_i + \|\Gamma^-(v)\|_1 \cdot (\delta_{v,z_v} - 1)$ .
20:  $\Psi := \text{DelFeature}(\Psi, \delta_{v,z_v})$ .
21:  $\Psi := \Psi \cdot \frac{c_{p_v}(z_v)}{c_v(z_v)}$ .
22: if  $z_v \in F_{p_v}$  then
23:   $\Psi := \text{AddFeature}(\Psi, \delta_{v,z_v})$ .
24: else
25:   $\Psi := \text{AddFeature}(\Psi, \delta_{v,q_{D-|F_{p_v}|}})$ .
function TreeSHAPFast
1:  $\phi = (0, 0, \dots, 0) \in \mathbb{R}^n$ .
2:  $\Psi := 0$ .
3: for  $i = 1$  to  $D$  do
4:   $\Psi := \text{AddFeature}(\Psi, 0)$ .
5: for  $y \in U$  do
6:   $H[y] := \emptyset$ 
7:   $\text{Traverse}(a_\rho)$ .
8:   $\text{Traverse}(b_\rho)$ .
9: return  $\phi$ 

```

the nearest ancestor of $w \in \mathcal{T}$ with $z_w = j$. One way to enable iterating through Q_v when v is processed bottom-up, is to maintain, for each feature $j \in U$, a global stack $H[j]$ containing all the nodes w such that $z_w = j$ and $\text{TraverseFast}(g_{w,j})$ has not yet completed. The stack elements are sorted using the pre-order of the nodes of v , so that the node w with the highest pre-order is at the top of $H[z_w]$. The stack can be updated in $O(1)$ time whenever a recursive call starts. Observe that $v \in H[z_v]$ when $\text{TraverseFast}(v)$

has started but has not yet finished. Now, given $H[z_v]$, it is enough to note that Q_v equals precisely the set of elements of $H[z_v]$ that lie higher than v . Thus, one can indeed iterate through Q_v in $O(|Q_v|)$ time as desired. Moreover, Q_v constitutes precisely the set of elements that have to be popped from the stack $H[z_v]$ when $\text{TraverseFast}(v)$ returns. The asymptotic cost of popping stack elements can be charged to the corresponding pushes and thus can be neglected. \square

Finally, we show that, roughly speaking, the same recursive relation as in Lemma 4 can be applied to the values $\Gamma(v)_k$ in order to obtain the required values $\Phi^-(v)$.

Lemma 8. *Let $\Gamma^-(v)_k = \sum_{l \in \mathcal{L}_v} f(l) \cdot \phi(l, F_l^* \setminus \{z_v\}, k)$. For any $l \in \mathcal{L}_v$ and $k \in \{0, \dots, D\}$ we have:*

$$\Gamma(v)_k = \frac{D-k}{D+1} \cdot \Gamma^-(v)_k + \frac{k[x_{z_v} \in I_{v,z_v}]}{(D+1)c_v(z_v)} \cdot \Gamma^-(v)_{k-1}.$$

Proof. Since $z_v \in F_l^*$ for all $l \in \mathcal{L}_v$, by Lemma 4, we have

$$\begin{aligned} \phi(l, F_l^*, k) &= \frac{D-k}{D+1} \left(\phi(l, F_l^* \setminus \{z_v\}, k) - \frac{k[x_{z_v} \in I_{l,z_v}]}{(D+1)c_l(z_v)} \phi(l, F_l^* \setminus \{z_v\}, k-1) \right) \\ &= \frac{D-k}{D+1} \left(\phi(l, F_l^* \setminus \{z_v\}, k) - \frac{k[x_{z_v} \in I_{v,z_v}]}{(D+1)c_v(z_v)} \phi(l, F_l^* \setminus \{z_v\}, k-1) \right). \end{aligned}$$

We obtain the desired equality by summing the above through all $l \in \mathcal{L}_v$. \square

For a convenient implementation, note that the vectors $\Gamma^-(v)_k$ are obtained from the corresponding vectors $\Gamma(v)_k$ in exactly the same way as $\Psi(v, F_v \setminus \{z_v\})$ was obtained from $\Psi(v, F_v)$ in the basic algorithm. Therefore, the functions `AddFeature`, `DelFeature` can be reused. More specifically, the following hold:

$$\Gamma(v) = \text{AddFeature}(\Gamma^-(v), \delta_{v,z_v}), \quad \Gamma^-(v) = \text{DelFeature}(\Gamma(v), \delta_{v,z_v}).$$

8 Other Feature Attribution Methods

Feature importance values summarize a complicated ensemble model and provide insight into what features drive the model's prediction. There can be various types of explanation methods to compute such values: model-dependent or model-agnostic methods, global or local explanation methods.

Explanation methods for trees: Global feature importance values are computed for an entire dataset in mainly three different ways. The basic global approach, *Split Count*, is to count the number of times a feature is used for splitting [13]. However, this method fails to account for the impacts of different splits. The *Gain* approach to feature importance [11] is to attribute the reduction of loss contributed by each split in each decision tree and it is widely used as the basis for feature selection methods [12, 21, 45]. Another commonly used approach, *Permutation*, is to randomly permute the data column corresponding to a feature in the test set and observe the change in the model's loss [10]. If the model is heavily dependent on the feature then permuting it should create a large increase in the model's loss.

These approaches are designed to estimate the global importance of a feature over an entire dataset, so they are not directly applicable to local explanations that are specific to each prediction. Local explanation methods for computing feature importance values for a single prediction are not well studied for trees. Only a couple of tree-specific local explanation methods were known previously. One is to just report the

decision path, which is not useful for large tree ensembles. The other one is by Saabas [44] which is a heuristic method that measures the difference in the model’s expected output. The Saabas method explains a prediction by following the decision path of the current input and attributing the differences in the expected output of the model to each of the features along the path. The expected value of every node in the tree is the average of the model output over the training samples going through that node. For explaining an ensemble model made up of a sum of many trees, the Saabas value for the ensemble is defined as the sum of the values for each tree.

As noted in [32], the feature importance values from the gain, split count, and Saabas methods are all inconsistent i.e., a model can be modified so that it relies more on a given feature, yet the importance assigned to that feature decreases.

Model-agnostic methods: One of the most common local explanation methods in deep learning literature is to take the gradient of the model’s output with respect to its inputs at the current sample or multiplying the gradient times the value of the input features. As depending entirely on the gradient of the model at a single point can often be misleading [48] various other methods have also been proposed [50, 56, 6, 48, 23, 5].

Model-agnostic methods on the other hand make no assumptions about the internal structure of the model and depend on the relationship between changes in the model inputs and model outputs. This is achieved by training a global mimic model to approximate the original model, then locally explaining the mimic model [7, 39]. Alternatively, the mimic model can be fit into the original model locally for each prediction. In the LIME method [41] the coefficients are used as an explanation for a local linear mimic model. In Anchors [42] the rules are used as the explanation for a local decision rule mimic model.

Recently, several methods for the local explanation of model predictions (such as LIME [41], DeepLIFT [48, 47], Layer-wise Relevance Propagation [6], and three methods from cooperative game theory: Shapley regression values [30], Shapley sampling values [51], and Quantitative Input Influence [15]) are unified into a single class of *additive feature attribution methods* [33]. This class contains methods that explain a model’s output as a sum of real values attributed to each input feature. It is of particular interest as there is a unique optimal explanation approach in the class that satisfies three desirable properties: local accuracy, missingness, and consistency [43, 46]. *Local accuracy* (also called *Efficiency* or *Completeness*) means that the sum of the feature attributions is equal to the output of the function we want to explain. *Missingness* (also called *Sensitivity*, or *Null-player axiom*) means that missing features are given no importance and *Consistency* (also called *Monotonicity*) means that if a feature has a larger impact on the model after a change then the attribution assigned to that feature can only increase.

One can use model-agnostic local explanation methods to explain tree models however their dependence on post-hoc modeling of an arbitrary function can make them slow or might suffer from sampling variability for models with many input features [31]. Although such methods are often practical for individual explanations, but can quickly become impractical for explaining entire datasets.

9 Conclusions

The contribution of this paper is twofold. First, we have developed new and more efficient algorithms for computing feature importance measures for tree ensemble models that are based on Banzhaf and Shapley values. These results improve the running time of previously known methods. Second, we present the first extensive comparison between Shapley and Banzhaf values. We observe that both methods deliver explanations of essentially the same strength by returning almost the same ordering of features. However, these experimental results indicate that Banzhaf values have several important advantages over Shapley values,

i.e., allow for faster algorithms as well as these algorithms make much lower numerical errors. As argued in the introduction, one should not base his decision on which index to use based on axiomatic characterizations, and other aspects should be considered. In particular, our study has delivered two important arguments for the usage of Banzhaf values.

References

- [1] BOSTON dataset.
- [2] FLIGHTS dataset.
- [3] HEALTH INSURANCE dataset.
- [4] SHAP python package.
- [5] M. Ancona, E. Ceolini, C. Öztireli, and M. Gross. Towards better understanding of gradient-based attribution methods for deep neural networks. In *ICLR*, 2018.
- [6] S. Bach, A. Binder, G. Montavon, F. Klauschen, K. Müller, and W. Samek. On pixel-wise explanations for non-linear classifier decisions by layer-wise relevance propagation. *PLoS ONE*, 10, 2015.
- [7] D. Baehrens, T. Schroeter, S. Harmeling, M. Kawanabe, K. Hansen, and K.-R. Müller. How to explain individual classification decisions. *Journal of Machine Learning Research*, 11(61):1803–1831, 2010.
- [8] F. Barthélémy, M. Martin, and V. Merlin. On the performance of the Shapley Shubik and Banzhaf power indices for the allocations of mandates. THEMA Working Papers 2007-25, THEMA.
- [9] N. Bordag, E. Zügner, P. López-García, S. Kofler, M. Tomberger, A. Al-Baghdadi, J. Schweiger, Y. Erdem, C. Magnes, S. Hidekazu, W. Wadsak, B.-T. Erxleben, and B. Prietl. Towards fast, routine blood sample quality evaluation by probe electrospray ionization (pesi) metabolomics. *medRxiv*, 2021.
- [10] L. Breiman. Random forests. *Machine Learning*, 45:5–32, 2004.
- [11] L. Breiman, J. H. Friedman, R. A. Olshen, and C. J. Stone. *Classification and Regression Trees*. CRC Press, 1984.
- [12] S. Chebrolu, A. Abraham, and J. Thomas. Feature deduction and ensemble design of intrusion detection systems. *Comput. Secur.*, 24:295–307, 2005.
- [13] T. Chen and C. Guestrin. XGBoost: A scalable tree boosting system. In *Proceedings of the 22nd ACM SIGKDD International Conference on Knowledge Discovery and Data Mining*, pages 785–794. ACM, 2016.
- [14] A. Datta, A. Datta, A. D. Procaccia, and Y. Zick. Influence in classification via cooperative game theory. In *Proceedings of the 24th International Conference on Artificial Intelligence, IJCAI’15*, page 511–517. AAAI Press, 2015.
- [15] A. Datta, S. Sen, and Y. Zick. Algorithmic transparency via quantitative input influence: Theory and experiments with learning systems. *IEEE Symposium on Security and Privacy (SP)*, pages 598–617, 2016.
- [16] X. Deng and C. H. Papadimitriou. On the complexity of cooperative solution concepts. *Math. Oper. Res.*, 19(2):257–266, 1994.
- [17] K. Dowding. Power: A philosophical analysis, 2nd edition. *Contemporary Political Theory*, 2, 10 2003.

- [18] P. Dubey and L. S. Shapley. Mathematical properties of the banzhaf power index. *Mathematics of Operations Research*, 4(2):99–131, 1979.
- [19] J. H. Friedman. Greedy function approximation: A gradient boosting machine. *Ann. Statist.*, 29(5):1189–1232, 10 2001.
- [20] S. Hart. *Shapley Value*, pages 210–216. Palgrave Macmillan UK, London, 1989.
- [21] V. A. Huynh-Thu, A. Irrthum, L. Wehenkel, and P. Geurts. Inferring regulatory networks from expression data using tree-based methods. *PLoS ONE*, 5, 2010.
- [22] D. Janzing, L. Minorics, and P. Blöbaum. Feature relevance quantification in explainable AI: A causal problem. In *The 23rd International Conference on Artificial Intelligence and Statistics, AISTATS*, volume 108, pages 2907–2916. PMLR, 2020.
- [23] P. Kindermans, K. T. Schütt, M. Alber, K. Müller, D. Erhan, B. Kim, and S. Dähne. Learning how to explain neural networks: Patternnet and patternattribution. In *ICLR*, 2018.
- [24] L. Á. Kóczy. *Measuring Voting Power: The Paradox of New Members vs. the Null Player Axiom*, pages 67–78. Springer Berlin Heidelberg, 2009.
- [25] S. Kurz. *Which Criteria Qualify Power Indices for Applications? A Comment to 'The Story of the Poor Public Good Index'*. SSRN.
- [26] A. Laruelle. On the choice of a power index. Working papers. Serie AD, Instituto Valenciano de Investigaciones Económicas, S.A. (Ivie), 1999.
- [27] A. Laruelle and F. Valenciano. Shapley-Shubik and Banzhaf Indices Revisited. *Mathematics of Operations Research*, 26(1):89–104, February 2001.
- [28] D. Leech. An empirical comparison of the performance of classical power indices. *Political Studies*, 50(1):1–22, 2002.
- [29] E. Lehrer. An axiomatization of the banzhaf value. *International Journal of Game Theory*, 17(2):89–99, Jun 1988.
- [30] S. Lipovetsky and M. Conklin. Analysis of regression in game theory approach. *Applied Stochastic Models in Business and Industry*, 17:319–330, 2001.
- [31] S. M. Lundberg, G. Erion, H. Chen, A. DeGrave, J. M. Prutkin, B. Nair, R. Katz, J. Himmelfarb, N. Bansal, and S.-I. Lee. From local explanations to global understanding with explainable AI for trees. *Nature Machine Intelligence*, 2(1):56–67, Jan 2020.
- [32] S. M. Lundberg, G. G. Erion, and S.-I. Lee. Consistent individualized feature attribution for tree ensembles. *arXiv preprint arXiv:1802.03888*, 2018.
- [33] S. M. Lundberg and S.-I. Lee. A unified approach to interpreting model predictions. In *Advances in Neural Information Processing Systems*, volume 30, pages 4765–4774. Curran Associates, Inc., 2017.
- [34] Y. Matsui and T. Matsui. NP-completeness for calculating power indices of weighted majority games. *Theor. Comput. Sci.*, 263:305–310, 2001.

- [35] J. A. Momo Kenfack, B. Tchantcho, and B. P. Tsague. On the ordinal equivalence of the johnston, banzhaf and shapley–shubik power indices for voting games with abstention. *International Journal of Game Theory*, 48(2):647–671, Jun 2019.
- [36] N. Patel, M. Strobel, and Y. Zick. High dimensional model explanations: an axiomatic approach, 2020.
- [37] F. Pedregosa, G. Varoquaux, A. Gramfort, V. Michel, B. Thirion, O. Grisel, M. Blondel, P. Prettenhofer, R. Weiss, V. Dubourg, J. Vanderplas, A. Passos, D. Cournapeau, M. Brucher, M. Perrot, and E. Duchesnay. Scikit-learn: Machine learning in Python. *Journal of Machine Learning Research*, 12:2825–2830, 2011.
- [38] H. N. Pham, T. T. Do, K. Y. J. Chan, G. Sen, A. Han, P. Lim, T. S. L. Cheng, Q. H. Nguyen, B. P. Nguyen, and M. C. H. Chua. Multimodal detection of parkinson disease based on vocal and improved spiral test. *2019 International Conference on System Science and Engineering (ICSSE)*, pages 279–284, 2019.
- [39] G. Plumb, D. Molitor, and A. S. Talwalkar. Model agnostic supervised local explanations. In *Advances in Neural Information Processing Systems*, volume 31, pages 2515–2524. Curran Associates, Inc., 2018.
- [40] K. Prasad and J. S. Kelly. NP-completeness of some problems concerning voting games. *International Journal of Game Theory*, 19(1):1–9, 1990.
- [41] M. T. Ribeiro, S. Singh, and C. Guestrin. Why should I trust you?: Explaining the predictions of any classifier. *Proceedings of the 22nd ACM SIGKDD International Conference on Knowledge Discovery and Data Mining*, 2016.
- [42] M. T. Ribeiro, S. Singh, and C. Guestrin. Anchors: High-precision model-agnostic explanations. In *Proceedings of the AAAI Conference on Artificial Intelligence*, volume 32, 2018.
- [43] A. Roth. The shapley value : essays in honor of Lloyd S. Shapley. *Cambridge University Press*, 1988.
- [44] A. Saabas. Treeinterpreter python package.
- [45] M. Sandri and P. Zuccolotto. A bias correction algorithm for the gini variable importance measure in classification trees. *Journal of Computational and Graphical Statistics*, 17:611 – 628, 2008.
- [46] L. S. Shapley. A Value for n-Person Games. *Contributions to the Theory of Games* 2.28, pages 307–317, 1953.
- [47] A. Shrikumar, P. Greenside, and A. Kundaje. Learning important features through propagating activation differences. In *Proceedings of the 34th International Conference on Machine Learning, ICML*, volume 70, pages 3145–3153. PMLR, 2017.
- [48] A. Shrikumar, P. Greenside, A. Shcherbina, and A. Kundaje. Not just a black box: Learning important features through propagating activation differences. *ArXiv*, abs/1605.01713, 2016.
- [49] J. Sliwinski, M. Strobel, and Y. Zick. Axiomatic characterization of data-driven influence measures for classification. *Proceedings of the AAAI Conference on Artificial Intelligence*, 33(01):718–725, Jul. 2019.

- [50] J. T. Springenberg, A. Dosovitskiy, T. Brox, and M. A. Riedmiller. Striving for simplicity: The all convolutional net. *CoRR*, abs/1412.6806, 2015.
- [51] E. Štrumbelj and I. Kononenko. Explaining prediction models and individual predictions with feature contributions. *Knowl. Inf. Syst.*, 41(3):647–665, 2014.
- [52] M. Sundararajan and A. Najmi. The many shapley values for model explanation. In *Proceedings of the 37th International Conference on Machine Learning ICML*, volume 119, pages 9269–9278. PMLR, 2020.
- [53] M. Sundararajan, A. Taly, and Q. Yan. Axiomatic attribution for deep networks. In *Proceedings of the 34th International Conference on Machine Learning, ICML*, volume 70, pages 3319–3328. PMLR, 2017.
- [54] B. Wang, S.-d. Fan, P. Jiang, H.-h. Zhu, T. Xiong, W. Wei, and Z.-l. Fang. A novel method with stacking learning of data-driven soft sensors for mud concentration in a cutter suction dredger. *Sensors*, 20(21), 2020.
- [55] R. J. Weber. Probabilistic values for games. *The Shapley Value. Essays in Honor of Lloyd S. Shapley*, pages 101–119, 1988.
- [56] M. D. Zeiler and R. Fergus. Visualizing and understanding convolutional networks. In *ECCV*, 2014.